8-2004

Dose Analysis by Radiation Treatment Planning System (TPS) Software Vs. Thermoluminescent Dosimeters Output

Carlos Eugene Corredor
University of Tennessee - Knoxville

To the Graduate Council:

I am submitting herewith a thesis written by Carlos Eugene Corredor entitled "Dose Analysis by Radiation Treatment Planning System (TPS) Software Vs. Thermoluminescent Dosimeters Output." I have examined the final electronic copy of this thesis for form and content and recommend that it be accepted in partial fulfillment of the requirements for the degree of Master of Science, with a major in Nuclear Engineering.

Laurence Miller, Major Professor

We have read this thesis and recommend its acceptance:

Lawrence Townsend, Ronald Pevey

Accepted for the Council:
Carolyn R. Hodges

Vice Provost and Dean of the Graduate School

(Original signatures are on file with official student records.)

To the Gradate Council:

I am submitting herewith a thesis written by Carlos Eugene Corredor entitled "Dose Analysis by Radiation Treatment Planning System (TPS) Software Vs. Thermoluminescent Dosimeters Output." I have examined the final paper copy of this thesis for form and content and recommend that it be accepted in partial fulfillment of the requirements for the degree in Masters of Science, with a major in Nuclear Engineering.

Laurence Z Miller

Laurence Miller, Major Professor

We have read this thesis and recommend it's acceptance:

Lawrence Townsend

Ronald E Pevey

Ronald Pevey

Acceptance for the Council:

Vice Chancellor and Dean of Graduate Studies

Dose Analysis by Radiation Treatment Planning System (TPS) Software Vs. Thermoluminescent Dosimeters Output

A Thesis

Presented for the

Master of Science Degree

The University of Tennessee, Knoxville

Carlos Eugene Corredor

August 2004

DEDICATION

This thesis is dedicated to my wife, Adriana and to my children Christopher and Ana Milena, who with their love and patience have guided me and supported me during my educational endeavors. To my father Carlos Fransisco, and my mother Shirley M., who have always instilled in me, the importance of education, as a tool in achieving my personal and professional goals.

ACKNOWLEDGEMENTS

I would like to acknowledge my major Professor Dr. Larry Miller, for his wonderful support, patience and understanding while working on my research in thermoluminescent dosimetry. Dr. Miller's knowledge and wisdom have provided me with the right tools that are needed to succeed at this institution.

I would like to thank the United States Army for providing me the trust and privilege of receiving a graduate level education. It is an honor to serve the United States Army and my country. An educated Army makes a stronger Army. I would like to mention as well the wonderful support that Bill Harris and his staff at the U.S. Army Radiation Standards and Dosimetry Laboratory, provided me during my research time at their facility.

I would like to mention as well the support provided to me by the staff at the Radiation Therapy Center, Baptist Memorial Hospital, Knoxville, Tennessee. Mark and Mat thank you very much for your wonderful expertise.

Finally, I would like to thank the wonderful intellectual and mental support of my graduate peers Robert Schlitz, Ravichandran Ramachandran, Brian Tylor, Nathan Delauder, Avijit Paul and Vijaya Kantubhukta . Working with all of you has been a pleasure. Your wonderful sense of humor and understanding helped me maintain my sanity during unforgettable crisis events.

ABSTRACT

Solid tumors are often treated with external beams of photons generated by bremsstrahlung radiation. These beams are shaped and filtered to optimize dose to specific regions defined by the treatment plans, which may involve irradiations from multiple angles. It is important that doses to healthy tissue not exceed tolerance doses and that the dose to the tumor be maximized. To accomplish these objectives, commercially available three-dimensional treatment planning software (TPS) is used to calculate doses to healthy tissue and to the tumor. It is generally believed that these commercial software packages calculate doses to the patient to within a few percent. The main objective of this study is to examine this claim. In order to determine the validity of the dose, calculations obtained from the TPS are compared with the dose response recorded by thermoluminescent dosimeters (TLD's) that were initially introduced in an Anthropomorphic Radiation Therapy (ART) phantom. Before inclusion into the ART Phantom, forty-two TLD's were properly calibrated using an NIST Co-60 source. The calibration of the TLD's took place at the United States Army Dosimetry Center, Redstone Arsenal, Alabama.

The radiation therapy system utilized in this study is the linear accelerator (LINAC) located at Baptist Cancer Center, Knoxville, TN. The LINAC was set to establish a prescription dose of 180 cGy to the pelvic region of the ART Phantom where the mock tumor was located. Analysis of the data reveals that 37 percent of the data calculated by the TPS differ from the dose response by the TLD-100s by more than 5%, with the majority of difference taking place at locations close to the emulated tumor, which seem to be due to inhomogeneities in the ART phantom.

Table of Contents

Chapter **Page**

1. Introduction 1

1.1 Introduction and General Information 1

1.2 Objectives of the Study 1

1.3 Purpose of the Research Study 2

1.4 Background information 2

2. Description of Research Equipment 7

2.1 Thermoluminescent dosimeters 7

2.1.1 Physics of TLDs 7

2.1.2 Additional Properties of TLDs 11

2.2 TLD-100 (LiF:Mg:Ti). Composition and Structure 12

2.3 Panasonic TLD system (UD-802AS) United States Dosimetry System.....13

2.4 The Alderson Radiation Therapy (ART) Anthropomorphic Phantom 16

2.5 The Thermoluminescent Dosimeter Reader 18

2.5.1 TLD Reader Specifications 20

2.5.2 TLD Reader software (WinRems©) 22

2.5.2.1 Time/Temperature profiles (TTP) 23

2.5.2.2 TLD Acquisition Parameter selection 23

2.6 Annealing Equipment 24

2.7 The Linear Accelerator (LINAC) Radiation Therapy System 26

2.8 Computerized Tomography (CT) X-Ray System 28

3. Experimental Methods 29

3.1 Calibration of TLD-100's (LiF:MG:Ti) 29

3.1.1 NIST Calibrated Radiation source..... 29

3.1.2 Exposure of TLD-100's to NIST Co-60 Source 31

Chapter **Page**

3.1.3 Element Correction Coefficient (ECC) 32
3.1.4 The Reader Correction Factor (RCF) 32
3.1.5 Dose Determination for each TLD-100 Chip 33
3.1.6 Workspace File Setup 34
3.1.6.1 Time Temperature Profile (TTP) 34
3.1.6.2 Acquisition Setup 35
3.1.7 TLD Calibration Reading 35
3.2 Linear Dose Response 35
3.3 Patient Treatment planning of the Art Phantom 37
3.4 TLD Setup in the ANDRO Anthropomorphic Phantom 39
3.5 ART Phantom setup and Exposure 41
3.6 Comparison of Dose Response of the Panasonic TLDs and the TLD-100 ... 43

4. Data Analysis 47
4.1 Determination of linearity 47
4.2 Comparison Between Treatment Planning (TPS) System and TLD-100 49
4.3 Paired Data Analysis between TLD-100 and TPS 51
4.4 Pairwise Comparison between TLD-100 and Panasonic TLD's 62
5. Conclusions and Future Work 65
List of References 69
Appendices 73
Vita 85

List of Tables

Table 3.1 Calibration of TLD-100's (LiF:Mg:Ti) 36

Table 3.2 Data Used to Check Linearity 38

Table 3.3 Doses to TLD-100's in the ART Anthropomorphic Phantom..... 44

Table 3.4 Dose Comparison between TLD-100 and Panasonic TLDs..... 45

Table 4.1 Basic Statistical Measures for TLD-100, STP and their Difference 56

Table 4.2 Tests for Normality 57

Table 4.3 Paired Data Analysis between TLD-100 and TPS 60

Table 4.4 Levene's Test for Homogeneity of dose Variance Between TLD-100 and TPS 61

Table 4.5 Table T-Tests for Means 61

Table 4.6 Levene's Test for Homogeneity of Dose Variance 64

Table 4.7 The T-Test Procedure 64

List of Figures

Figure 1. TLD discrete energy bands 8

Figure 2. Scintillation process of a TLD 9

Figure 3. Size of TLD's compared with a quarter 12

Figure 4. Panasonic TLD system (UD-802AS) 14

Figure 5. The ART Anthropomorphic Phantom 17

Figure 6. Transverse cut of an ART Phantom slice with different forms of TLD's.... 19

Figure 7. Harshaw TLD Reader 21

Figure 8. Glow Curve from Harshaw 3500 TLD Reader 24

Figure 9. PTW-TLDO Annealing Oven 25

Figure 10. Varian CLINAC 27

Figure 11. Co-60 and Cs-137 Sources. J.L Shepherd Model 81-22T 30

Figure 12. 3D dimensional view of Mock Tumor on the ART anthropomorphic Phantom 40

Figure 13. CT Cross-sectional view of the ART Phantom and diagram of TLD Location 42

Figure 14. Dose Response Linearity of TLD-100 48

Figure 15. Dose Residual values Vs. Predicted values 48

Figure 16. Dose Comparison between the TPS and TLD-100 52

Figure 17. Percent Difference between measured Dose and Calculated Dose 52

Figure 18. Comparison of Data Distribution between TLD-100 and the TPS 54

Figure 19. Distribution if the Difference between TLD-100 and TPS 54

Figure 20. Normal Probability Plot for the Difference Between the TLD-100 and the TPS..... 55

Figure 21. Normal Distribution of the Residuals of TLD-100 and the Panasonic TLD's..... 63

Chapter 1

Introduction

1.1. Introduction and General Information

One of the main goals in radiation therapy is the effective treatment of solid tumors through the use of external beams of photons that are generated by Bremsstrahlung radiation. In order to optimize the essential dose to a tumor that has been prescribed in a specific treatment plan, the photon beams delivered at multiple angles are shaped or filtered. It is important that doses to healthy tissue do not exceed tolerance doses and that the dose to the tumor be maximized. To accomplish these objectives, commercially available three-dimensional treatment planning software or treatment planning systems (TPS) are used to calculate doses incident to the tumor and to healthy tissues that are in the vicinity of the tumor. It is generally believed that these commercial software packages calculate doses through the patient to within a few percent.

1.2 Objectives of the Study

The main objective of this study was to examine this claim. In order to determine the validity of the dose calculations obtained from the TPS, an external beam treatment to the pelvic region of an anthropomorphic phantom is compared with the dose response recorded by thermoluminescent dosimeters (TLDs) introduced in the phantom. Included in this study is the determination of the effectiveness of the TLDs used in this study as compared to other TLD systems. The TLDs were compared to the dosimetry system that is utilized by the United States Army.

1.3 Purpose of the Research Study

The purpose of this study is to compare the dose calculated by the three-dimensional software developed by the Analytical Development Associates Corporation (ADAC) with the dose measured by a Lithium Fluoride TLD (TLD-100,). The use of TPS software has been incorporated in different medical linear accelerators (LINAC) systems used for radiation therapy since the mid 1960s. The software developed by ADAC that is used in this study is called "Pinnacle^3", and it aids physicians and oncologists in treatment planning and optimal dose calculations for the treatment of solid tumors. The TLD 100's are solid dosimeter chips made from a semiconductor material, more specifically Lithium Fluoride (LiF:Mg:Ti). The LiF TLDs are reusable and highly sensitive, with a range of exposure from a few mR to 200,000 R. TLD-100's are extensively used in radiation therapy for many purposes, e.g., skin dose calculations, internal doses, dose verification, etc.

1.4 Background information

Previous studies have been performed to verify the validity of the accuracy of treatment planning system (TPS) software. Of interest is a study performed by Dunscombe *et al* (1995), where a series of eight irradiations of an anthropomorphic phantom were performed to verify the validity of the TPS system software. The eight irradiations represented the typical treatment configurations that are routinely used in a radiation therapy center. The dose distribution in the phantom was determined using approximately 75 TLD-100 dosimeters and compared to the calculated dose that was

provided by the TPS. Additionally, dose gradient was also determined for the phantom. The dose gradients were divided into three sections: Low, medium and high.

In the study by Dunscombe *et al*, the accuracy of the measurements at the different configurations provided by the TLDs in the anthropomorphic phantoms were on the average within 3 % for an individual dose and the position of the TLD was within 3 mm or better of measurement points at the different dose gradients. In the Dunscombe study, they were also able to be in compliance with the calculated dose as specified by the criteria of acceptability described by Van Dyk *et al* (1993) for the low and high dose gradient region. However, values were not within compliance for the medium region. The non-compliance of the dose gradient for the medium region was attributed to certain uncertainties such as the possibility of operator error or improper use of measurement techniques for the study.

At the University of Texas in Houston, a study was also performed (Baird *et al.* 2000) on the verification of the dose calculations provided by a three dimensional TPS during tangential breast treatment. Traditionally, in the early treatment of breast cancer, a two dimensional TPS system is utilized. For small and medium breasted women the dose is delivered uniformly on the central axis plane of the breast. However, it was shown that for large breasted women there was an increase in hotspots (high dose), which can be attributed to the different changing contours of the breast. Because of the inhomogeneity of the dose that takes place during the treatment, the end result of the treatment provides a cosmetic concern for the patient being treated. A customized breast representing a large-breast was created using machinable wax and attached to an anthropomorphic phantom. In order to optimize the dose and to distribute it uniformly to the breast, a

three-dimensional TPS was used in order to reduce the hotspots that can be created using a two dimensional TPS. To measure the uniformity of the dose distribution at the axial midplane of the breast, radiographic film was utilized. Additionally TLD-100's were place in four locations of the breast to validate the dose distribution shown by the radiographic film. Film measurements and TLD-100 measurements were compared to the calculated dose provided by the three dimensional TPS for four types of treatment: Two optimized wedged beams at 6 and 18 Mega electron volts (MV) and two dimensional compensated beams at 6 and 18 MV. In order to distinguish photon energy needed to produce ionizing radiation in a LINAC and not by an electron beam, the abbreviation used is MV. For electrons the abbreviation is MeV.

Results of the study made by Baird et all (Baird *et al.* 2000), showed that the accuracy of the TLDs and the film were within 0.6 %. TLD dose errors were 0 to 3% and 0.5 to 1% for 6 and 18 MV respectively. Radiographic film dose was on the average 1.5% lower than the values expressed for the TLD-100's. The measured and calculated dose through the mid-plane area differed by ± 3% for both the TLDs and the radiographic film. Areas out of the mid-plane region did not show the accuracy shown in the mid-plane, either because of the limitations of the radiographic film or because of the dose calculation algorithm of the TPS in regions of inhomogeneities.

Finally, another study was performed (Waligorski *et al*, 2000) on the accuracy of a TPS entitled "Validation of a Radiotherapy Treatment Planning System Using an Anthropomorphic Phantom And Mts-N Thermoluminescent Detectors." This study is more within the realm of the research reported herein. The objective of Walgorski *et al.* was to determine the validation of several TPS, instead of just one of them. The TPS

calculated dose was compared to the dose measured by TLD-100's that were previously calibrated in a water phantom. All TLD-100's were placed inside an anthropomorphic phantom around a region of interest (ROI) in the pelvic area, and a treatment plan was created using external beams from a Co-60 radiation therapy system and a LINAC at 6 MV. Before initial exposure to any patient, positioning markers and a CT scan were also performed on the anthropomorphic phantom. This technique facilitates the positioning of the radiation therapy systems and repositioning of the phantom at a later time during future exposures. Using the scans and the positional markers and placing the phantom in the correct position, a dose of two Grays (Gy) was imparted to the ROI. Eleven measured points were observed and the calculated planned doses were compared to the measured dose provided by the TLD-100.

The relative difference shown in this study (Waligorski *et al*, 2000) was between -3.2 and 3.14 %, and -3.81 and 2.47 % for the Co-60 system and the LINAC system respectively. Standard deviation values for measured doses in the ROI were also calculated. The standard deviation values for the Co-60 treatment plans were 4.2 % and 5.2 %. For the LINAC system treatment plans the values were 3.6% and 5.2 % . The conclusion reached is that all values are within the recommendations set by the International Commission of Radiation Units and Measurements (ICRU). It is also expressed that additional studies should be performed using TLDs and anthropomorphic phantoms to verify the accuracy of TPS.

Few studies like these have been made to validate that TPS provide an accurate calculated dose, and few medical facilities have time to do this type of research. It should be routine that Quality Assurance (QA) and Quality Control (QC) programs be present in

medical facilities that provide radiation therapy treatment. This would ensure that an accurate dose is given to the patient. However, it is of interest that the calculated dose be verified against other detection systems that give an accurate measured dose, as is the case of properly calibrated TLDs.

Chapter 2

Description of Research Equipment

2.1 Thermoluminescent dosimeters

Thermoluminescent dosimeters (TLDs) are solid semiconductors that, if heated after being exposed to radiation, will emit visible light that is proportional to the amount of radiation to which they were initially exposed. Because of this capability, TLDs have many uses in industry and in the medical field. One of the main uses of TLDs is monitoring the radiation dose to which occupational workers in hospitals, research facilities, and nuclear reactors have been exposed. Other uses can be to determine actual doses administered at either skin or body cavities of patients undergoing radiation therapy. Additionally, they can be used for environmental monitoring in the processing, storage or disposal of radioactive material in compliance with federal and state laws.

2.1.1 Physics of TLDs

TLDs are solid crystalline materials that are semiconductors. Semiconductors, in general, conduct electricity only under certain conditions compared to conductors that fully conduct electricity (e.g. iron) or to those materials that do not conduct any electricity at all, which are called insulators (e.g. plastic). Semiconductors conduct electricity depending on the temperature. At absolute zero they do not conduct. However, as temperature increases the conductivity of TLDs also increases. The process of thermoluminescence of TLDs takes place by initially absorbing radiation, whose energy is trapped in the TLD. The trapped energy can then be released if the TLD is exposed to heat. The energy that is released is delivered in the form of visible light.

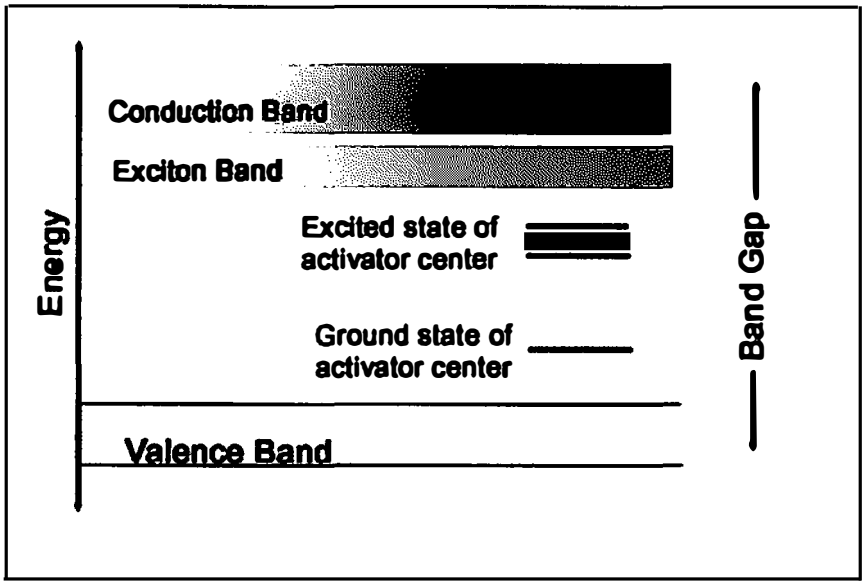

Figure 1. TLD discrete energy bands

Source: Dr. Larry Miller, Lecture Notes, Nuclear Engineering Department. University of Tennessee

A more detailed analysis of this process can be understood by looking at a TLD at the atomic level. In semiconductors, electrons can located at discrete energy bands. The two main bands we are concerned with are the valence band and the conduction band. Electrons are distributed spatially in the TLD crystal depending on their energy either in the valence or in the conduction band (Figure 1).

At the valence band are those electrons that are located at the lattice sites of the crystal. Electrons that have sufficient energy to migrate through the crystal will be located at the conduction band. To make an electron located at the valence band jump to

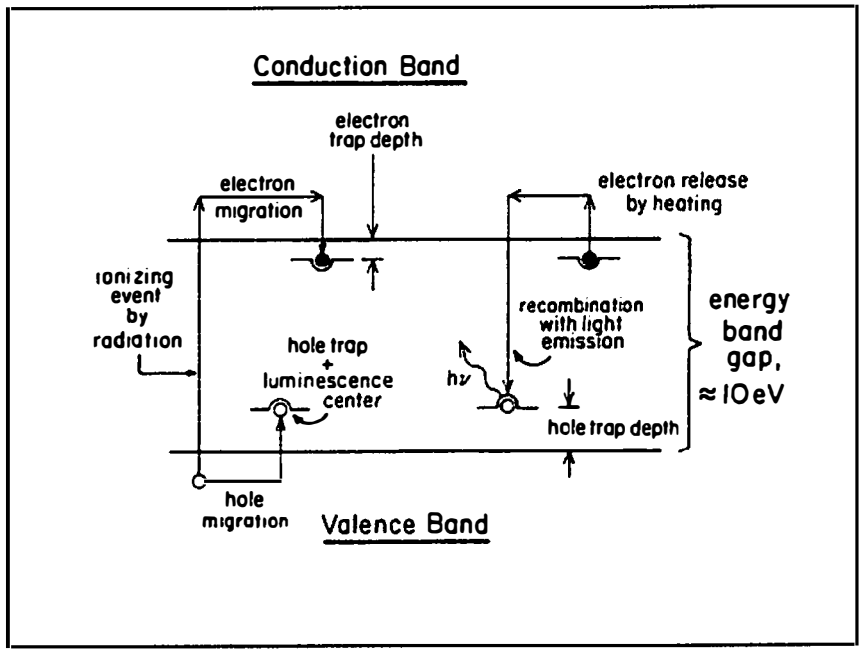

Figure 2. Scintillation process of a TLD
Source: Dr. Larry Miller, Lecture Notes, Nuclear Engineering Department. University of Tennessee

the conduction band, enough energy must be provided to overcome the energy gap of 10 electron Volts (eV) between the bands.

When TLDs are exposed to radiation, electrons located in the valence band are excited and jump above the band gap and into the conduction band, leaving behind an empty space or hole. This creates what is called an electron-hole pair (Figure 2.). On the energy borderlines of the valence band and the conduction band with the energy gap, two additional energy sites are present. The excited activator site is located close to the lower energy border of the conduction band. Electrons located in the conduction band tend to drift to this site. On the other hand, the ground activator site is close to the upper energy limit of the valence band and positive holes will drift to this site. Electrons and holes will

stay in place as long as the TLD is not heated. If the TLD is heated, then the electron will move out of the conduction band and rejoin the positive hole, emitting visible light.

The visible light emitted is proportional to the amount of radiation, to which the TLD was exposed to. A photomultiplier tube (PMT) converts the light into an electrical charge that is sufficiently amplified as to be read by a meter or a computerized system. The electrical charge, usually expressed in nanocoulombs, is also considered to be proportional to the radiation or the absorbed dose that initially exposed the TLD.

The light intensity or brightness produced by combining an electron and a positive hole is known as a glow peak. Glow peaks can be fully or partially resolved. The integration of all the glow peaks produced by the sum of all electrons escaped is known as a glow curve (Figure 7). Both glow peaks and glow curves can be observed in the output that is created by a TLD Reader and the computerized system that is attached to the reader.

An additional factor to consider when heating a TLD is the probability of escape of the electron from the conduction band. This probability of escape is related to two main parameters. One is the energy level in which the electron was trapped and the second is the amount of heat that is imparted. Electrons that are more deeply trapped will require a higher temperature to be released than electrons that are in shallow traps, which will require lower temperature.

$$p = \alpha * e^{-E/kT} \qquad (2.1)$$

This probability of escape can be expressed mathematically using the Randall-Wilkins theory (Equation 2.1), where p is the probability of escape of the electron, α is a

constant called the frequency factor, E is energy depth of the trap, k is the Boltzmann constant and T is the temperature in degrees Kelvin. From this formula we can ascertain that for a given T, the probability of escape, p, will decrease with increasing energy to the energy depth of the trap. But at any given E, increasing T will also increase p. Thus, it can be observed that if T is not increased when energy is high, the probability of escape is reduced.

Glow peaks are produced depending on the energy depths at which the different electrons were trapped. A maximum glow peak will occur at the highest cutoff temperature that was applied to the element. This highest glow peak will release a certain amount of visible radiation depending on the rate at which heat is applied to the TLD. If temperature is increased at a high rate per unit time, then the glow peak will have a smaller height in the distribution of that peak. If the temperature rate increase is less per unit time, then the height of the glow peak will be larger. Therefore, when reading TLDs it is important to consider the appropriate linear heating rate in order to achieve an optimum light emission and an effective integration of all glow peaks under the glow curve.

2.1.2 Additional Properties of TLDs

There are many forms of TLDs that are used in industry, and the main properties that are considered when trying to select the appropriate TLDs are (Tsoulfanidis, 1995):

- A linear response over a large dose range.
- Perfect annealing that enables repetitive use of TLD.
- Resistance to fading
- Small size and ruggedness

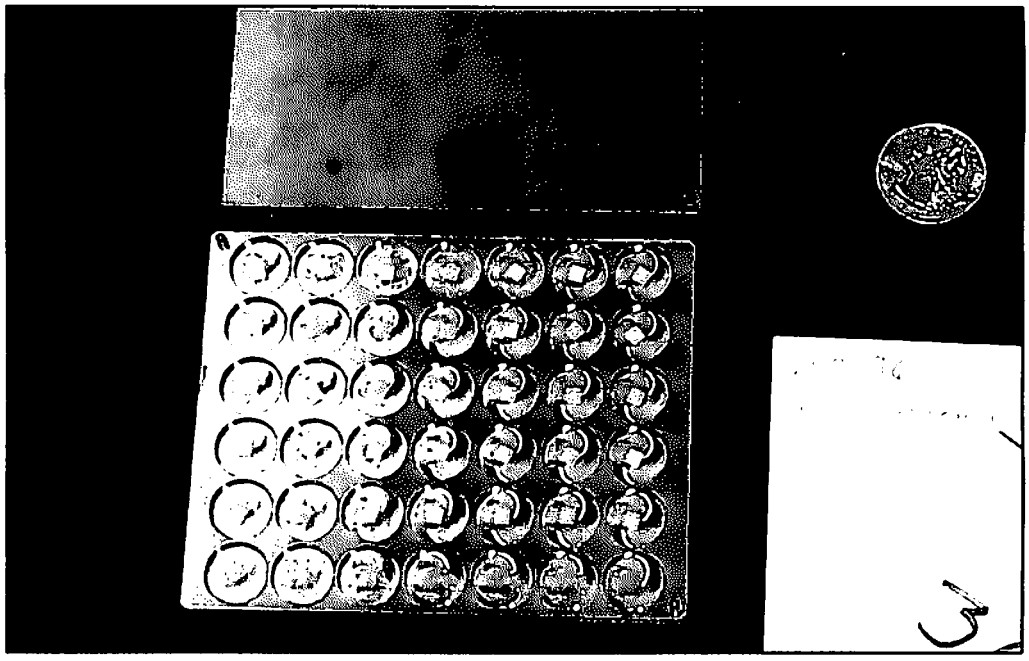

Figure 3. Size of TLDs compared with a quarter

2.2 TLD-100 (LiF:Mg:Ti). Composition and Structure

The TLD 100's used in this research are a product of the Harshaw Chemical Company. They are solid semiconductor crystals (Figure 3) composed of Lithium Fluoride (92.6 Li-7, 7.4 Li-6). TLDs are not usually pure and, in general added impurities are found in them. Impurities such as magnesium and titanium can be added to the TLD-100 to create new states in which additional holes and electrons may be found, increasing the conductivity of the TLD (Tsoulfanidis, 1995). The types of ionizing radiation that a TLD-100 typically responds to are x-ray, gamma, alpha and beta radiation and thermal neutrons.

TLD 100's show the properties mentioned above (Tsoulfanidis, 1995). TLD-100 are small chips with a size of approximately 0.125 square inches and a thickness of 0.035 inches. A comparison of the size of a TLD with that of a quarter can be observed in Figure 3, where 36 TLD-100 are placed in a copper planchet that is used in the annealing process of TLDs. The useful range of the TLD-100 is from 3 milliRoentgen (mR) to 10^5 Roentgen. The percent deviation for a first order calibation function of the TLD-100 is 5 to 10 % at higher doses and it increases at lower doses to values above 20 to 30 %.

2.3 Panasonic TLD system (UD-802AS). United States Army Dosimetry System

The Panasonic System UD-802As (Figure 4.) is composed of four TLD elements. Two are made of di-Lithium Tetra Boron Oxide ($Li_2B_4O_7$) and the other two are made of Calcium Sulfate ($CaSO_4$). The 4 TLD elements also show the typical properties that a good TLD should have (Tsoulfanidis, 1995). The dosimeters are read using a Panasonic UD-710A automatic thermoluminescent dosimeter readers with the results evaluated using a dose equivalent conversion algorithm.

Evaluation of the Panasonic TLD badges is performed with two procedures, which are performed in sequential order. First, the type of radiation is determined by calculating and comparing the TLD element ratios (E1 thru E4) to those ratios observed when radiation type and quality is known. Secondly, the dose at specific depths is calculated by multiplying the element response by a factor predetermined at the Dosimetry center which converts the badge reading into the dose equivalent at the shallow (7 mg/cm^2), eye (300 mg/cm^2), and deep (1000 mg/cm^2) tissue depths. The $CaSO_4$:Tm elements have an effective Z number greater than tissue, therefore, they over respond relative to tissue to

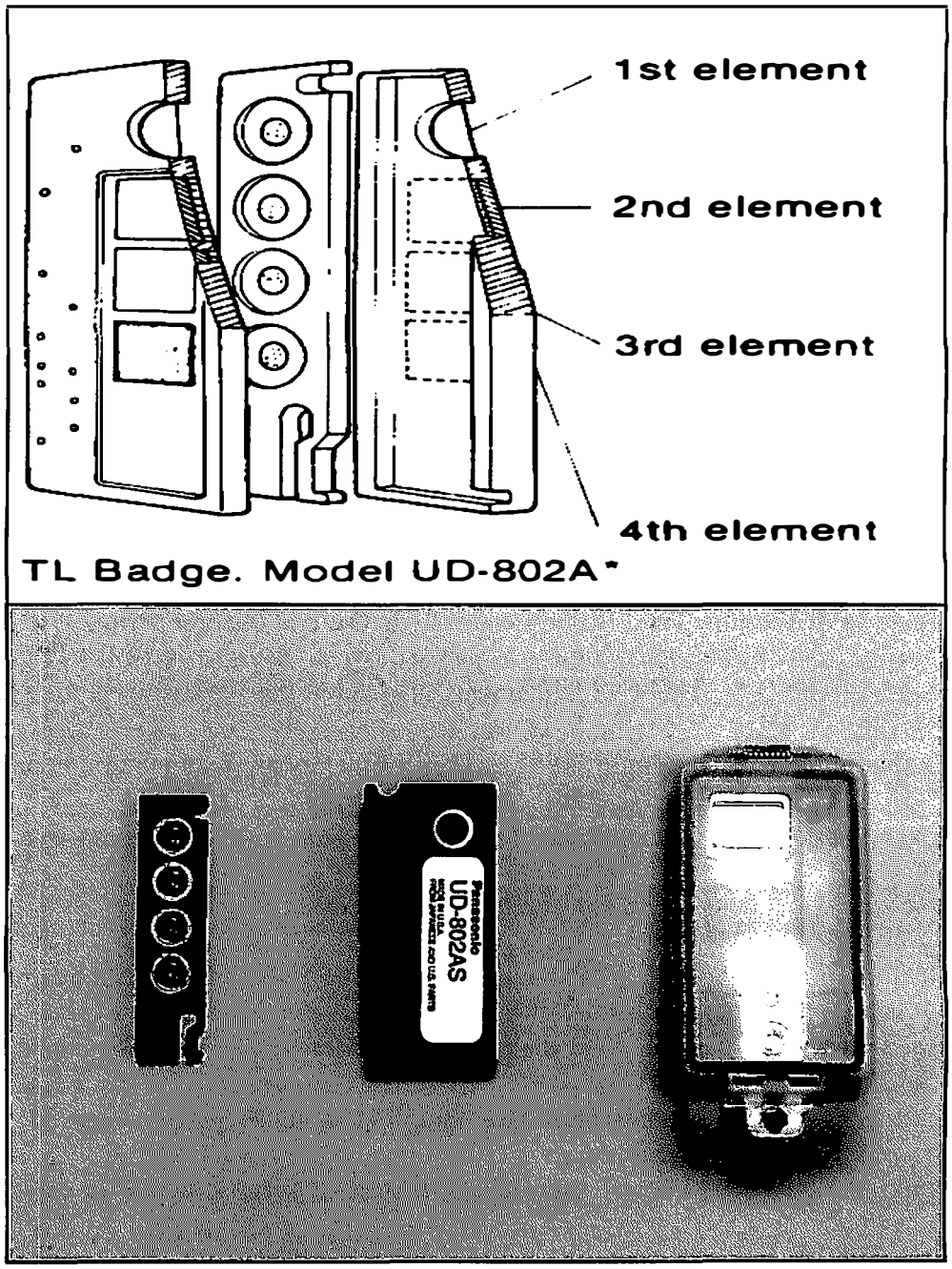

Figure 4. Panasonic TLD system (UD-802AS)

Source: U.S. Army Radiation Standards and Dosimetry Laboratory, Redtone Arsenal, AL, 2004

low energy photons. To assess photon energy, the algorithm calculates and compares the E3 to E4 ratio to those observed with a known radiation quality. After the algorithm determines the photon energy, the E2 element reading is multiplied by factors that convert the element response into the three different tissue depth doses: shallow dose, eye dose and deep dose.

The efficiency of the Army TLD system is tested on a routine basis at different energy levels, for photons, neutrons and beta particles. In order to ensure the best performance and quality service, the TLDs are sent to be reviewed for accuracy and efficiency on a yearly basis by the National Voluntary Laboratory Accreditation Program (NVLAP), which is a division of the National Institute of Standards and Technology (NIST). The latest review of the program took place in 2003 when the U.S. Army met all requirements established by NVLAP.

For this study we will be using dose exposures of 100 cGy or more. At this level of exposure, the percent deviation between measurement and calibration source of the accuracy of the U.S. Army Panasonic TLD, within a range of exposure of 10 cGy to 500 cGy, is about 3 %.

These TLD elements provide the flexibility and accuracy needed to evaluate the appropriate dose at different tissue depths and, therefore, they can be used to determine at the same time skin dose and whole body dose. The Panasonic TLD system is also used for determining dose to the thyroid gland or to determine a fetal dose for occupational workers that are expectant.

2.4 The Alderson Radiation Therapy (ART) Anthropomorphic Phantom

The ART phantom is used as a model of a human being. The phantom is shaped like a human, and is composed of materials that are equivalent to the different tissues and different organs that are found in a reference human person (Figure 5.). The ART phantom is used in this study to make dose comparisons between the TPS software and the TLD-100 measurements. The ART phantom is used in medical physics as well as in health physics for radiation protection purposes and it serves as a tool in determining the effective dose or effective dose equivalent to a human without the need to expose an actual person. By averaging the individual doses to organs and tissues with weight factors that are associated to their radiosensitivity, it leads to the determination of an effective dose equivalent for the phantom that can be applied to the human body (Shultis *et al*, 2000).

Since there is a geometrical similarity of the ART Phantom with a reference person's tissues and organs, medical terminology used to determine anatomically the positional view of a human subject can be extended for the positional views of the ART phantom. This positional view is quite helpful when determining the direction in which ionization radiation will impinge on the ART phantom.

Some of the positional views utilized in radiation therapy are:

- Anterior-Posterior View (AP): This is the view where the ionizing radiation exposure is from the front to the back at a right angle to the long axis of the phantom.
- Posterior-Anterior (PA) View: This view is from the back (Posterior) towards the front (Anterior) at a right angle to the long axis of the phantom or person .

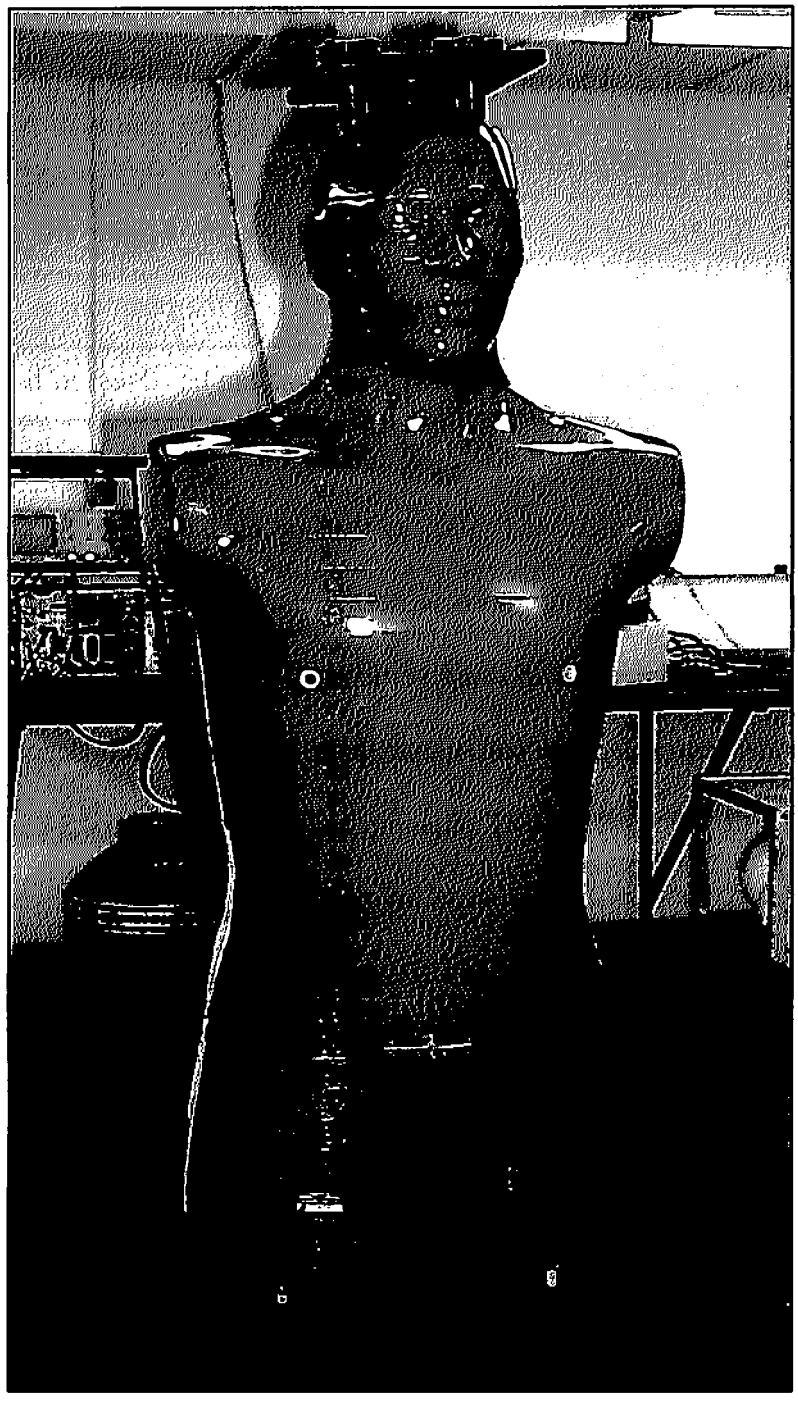

Figure 5. The ART Anthropomorphic Phantom

- Lateral (LAT): This view observes the phantom from either side at a right angle to the long axis of the phantom.
- Rotational View (ROT). The rotational view is a 360 view that is perpendicular to the long axis of the phantom (Shultis *et al*, 2000).
- Isotropic View (ISO). The best way to describe this is to imagine the phantom in a transparent sphere, where the region of interest (ROI) in the phantom is located in the middle of the sphere. The ISO view is any view that can be observed from any point on the surface of the sphere to the ROI.

The ART phantom is assembled in slices that are each 2.5 cm thick, and is held together by tie rods and tensioning knobs at both ends. A metal base is placed at the bottom of the ART Phantom so it can stand vertically (Figure 5.). Each slice is made up of materials that are equivalent to soft tissue, bone or lung tissue depending on the relative position of the slice. The ART phantom has an equivalent of 34 slices starting with slice number 1 on top of the head of the ART Phantom. Every slice has incorporated a grid of holes with plugs placed apart in a 3 X 3 cms pattern. The plugs and holes transverse the slice perpendicularly along the long axis of the phantom.
The plugs can be customized so they can accept different forms and shapes of TLDs (Figure 6). The TLD-100's for this study were placed in 37 locations on different slices located around the ROI.

2.5 The Thermoluminescent Dosimeter Reader

The Harshaw Corporation, a division of the Saint-Gobain Crystal and Detector Corporation, developed the manual TLD reader (Model 3500) used in this study. The

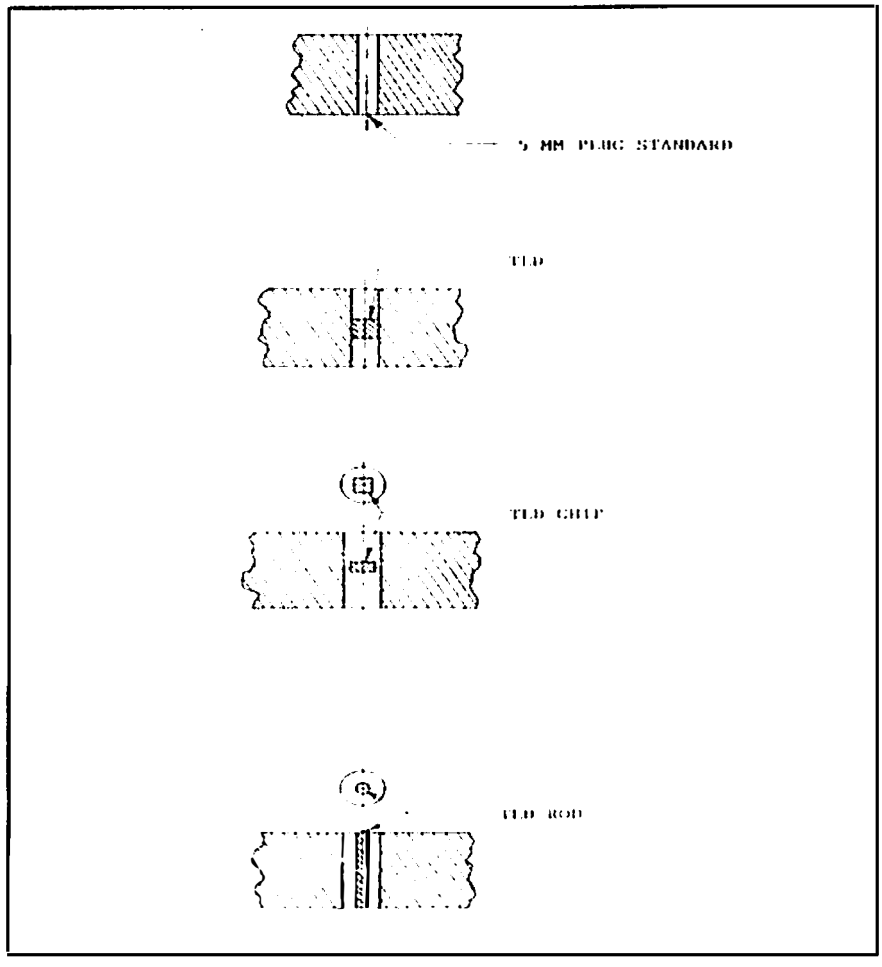

Figure 6. Transverse cut of an ART Phantom slice with different forms of TLDs.

Source: Radiology Support Devices, Long Beach CA , 1990

TLD reader can read individual TLD elements including rods, ribbons and chips. The system is attached to a personal computer where it interfaces with proprietary software developed by the Harshaw Corporation. The TLD reader (Figure 7) incorporates a single tray where the different forms of TLD elements can be read. It also includes a linear heating system and a PMT tube that measures the light output from the TLDs. The amplified signal is sent through the reader's electronics and transferred to the software for proper analysis of the output.

2.5.1. TLD Reader Specifications

The TLD Reader specifications are presented below (Bicron, 2004):

Radiation Measured:	Photon Energies above 5 Kilo Electron Volts (keV), thermal neutrons up to 100 MeV, and electron/Betas greater than 70 keV.
Range:	10 micro Grays (μGy) to 1 Gy (Linear); 1 Gy to 20 Gy (Supralinear).
Tissue Equivalence:	Near Tissue equivalence.
Fading:	Less than 20 % in three months without thermal pretreatment. 5 % in three months using initial preheat.
Residual Tl signal:	Over the range without annealing TLDs, less than 2 % is residual TL signal.
Reuse:	More than 500 times per dosimeter with a 10 % sensitivity Change.

Figure 7. Harshaw TLD Reader

Source: Thermo Electron Corp, Santa Fe, 2004

Preheat temperatures:	Up to 600 ^{o} C
Acquisition Temperature:	Up to 600 ^{o} C
Annealing Temperature:	Up to 600 ^{o} C

In order to reduce the potential emission of light that is not produced by the heating process of the TLDS (noise), and to eliminate any possible interferences between the PMT and the location of the planchet where the TLD is located, a flow of nitrogen at room temperature is passed over the PMT. The nitrogen flow for this study was preset at 5 standard cubic feet per hour (SCFH) with the gas regulator for the nitrogen tank set at a pressure of 200 Kilo-Pascals.

2.5.2 TLD Reader software (WinRems©)

Before any TLD element can be read, several parameters must be set in the software prior to the use of the 3500 Harshaw TLD reader. The software system provides the option of setting initial parameters before reading the TLD, the controls needed to operate the TLD reader system and a visual output of the glow curves to the PC system that results from reading the TLD. Additional options include exporting or printing the resulting numerical data, and the graphics. The software used with the TLD reader is a Microsoft© Windows Based program. In WinRems© you must create a working space file, which will set up several databases and text files within the working space, and which will hold output results during the TLD reading process. Before any readings can be done two main parameters in the Workspace file must be created: the Time/Temperature Profile and the TLD Acquisition parameter:

2.5.2.1 Time/Temperature profiles (TTP)

The TTP provides for the selection of predefined temperatures. A preheat time can be established in order to remove unnecessary shallow traps at very low temperatures. A linear heat rate can also be determined for an optimum light output. A post-anneal time can be created as well, where higher temperature heats are applied to the TLD in order to completely anneal or eliminate all traps so the TLD, can be reused.

Even though the system provides the capability of annealing the TLD, a separate annealing oven was used to clear the TLDs before the next use.

2.5.2.2 TLD Acquisition Parameter selection

Several options can be selected in order to facilitate the reading of the TLD. When considering reading TLDs, two correction factors must be established during the initial calibration of TLD. One is the correction for the TLD reader called the Reader Correction Factor (RCF) and the second is the TLD Element Correction Coefficient. These two factors will be discussed in later chapters when describing the process of calibration of the TLDs. If these two factors are known, they can be applied in the software before final reading of a TLD element. Also under acquisition one can include an automatic background subtraction, as well as a periodic testing of noise and a response to test light. For this study these last two were automatically determined every 10 TLDs. The RCF, the ECC's for each TLD element and the background were applied manually in this study and were not included in the acquisition parameter settings of the software.

One of the most important functions of the TLD reader software is the graphical and numerical output after reading a TLD as well as the analysis of the data represented.

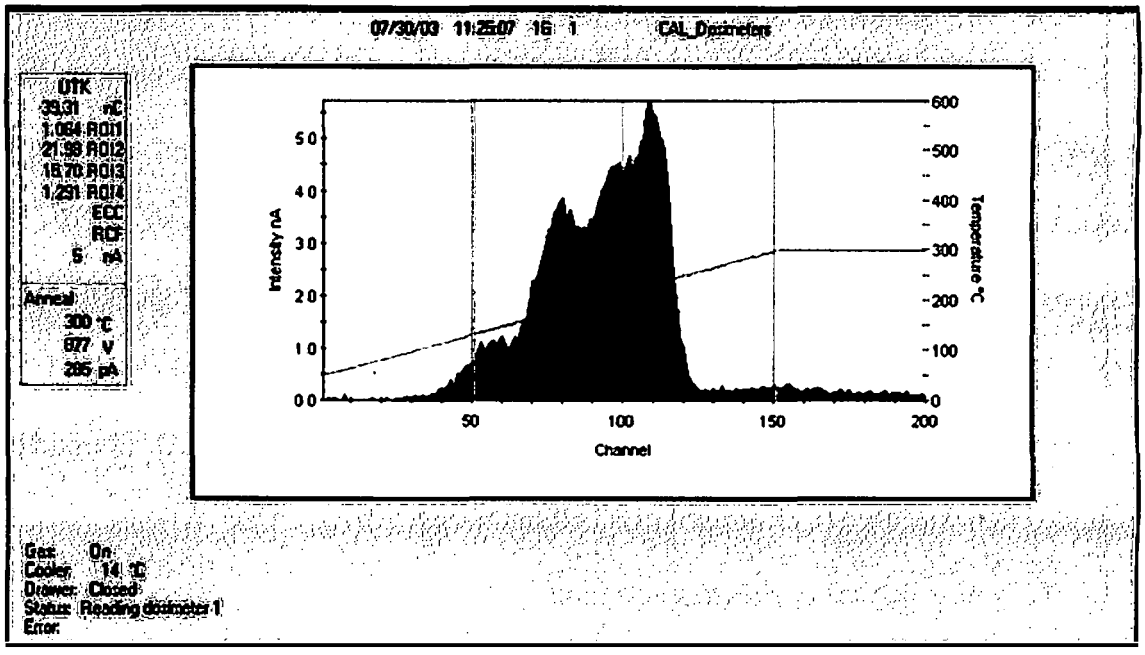

Figure 8. Glow Curve from Harshaw 3500 TLD Reader

Source: Carlos Corredor, University of Tennessee, Knoxville, TN 2003

Every readout provides a graph of the integrated glow curve as well as the integrated value of the charge produced. The glow curve as well as the electrical charge value can also be divided in ROI's for additional analysis. Figure 8 shows a typical glow curve output created by this software.

2.6 Annealing Equipment

For the process of annealing the TLD elements, the PTW-TLDO annealing oven manufactured by the PTW-Freiburg Corporation was used. The oven is specifically designed for the annealing process of TLDs. The PTW-TLDO annealing oven (Figure 9) has two program settings. Program 1 is designed for annealing before irradiation of TLDs.The second oven program is used for annealing TLDs after irradiation of the

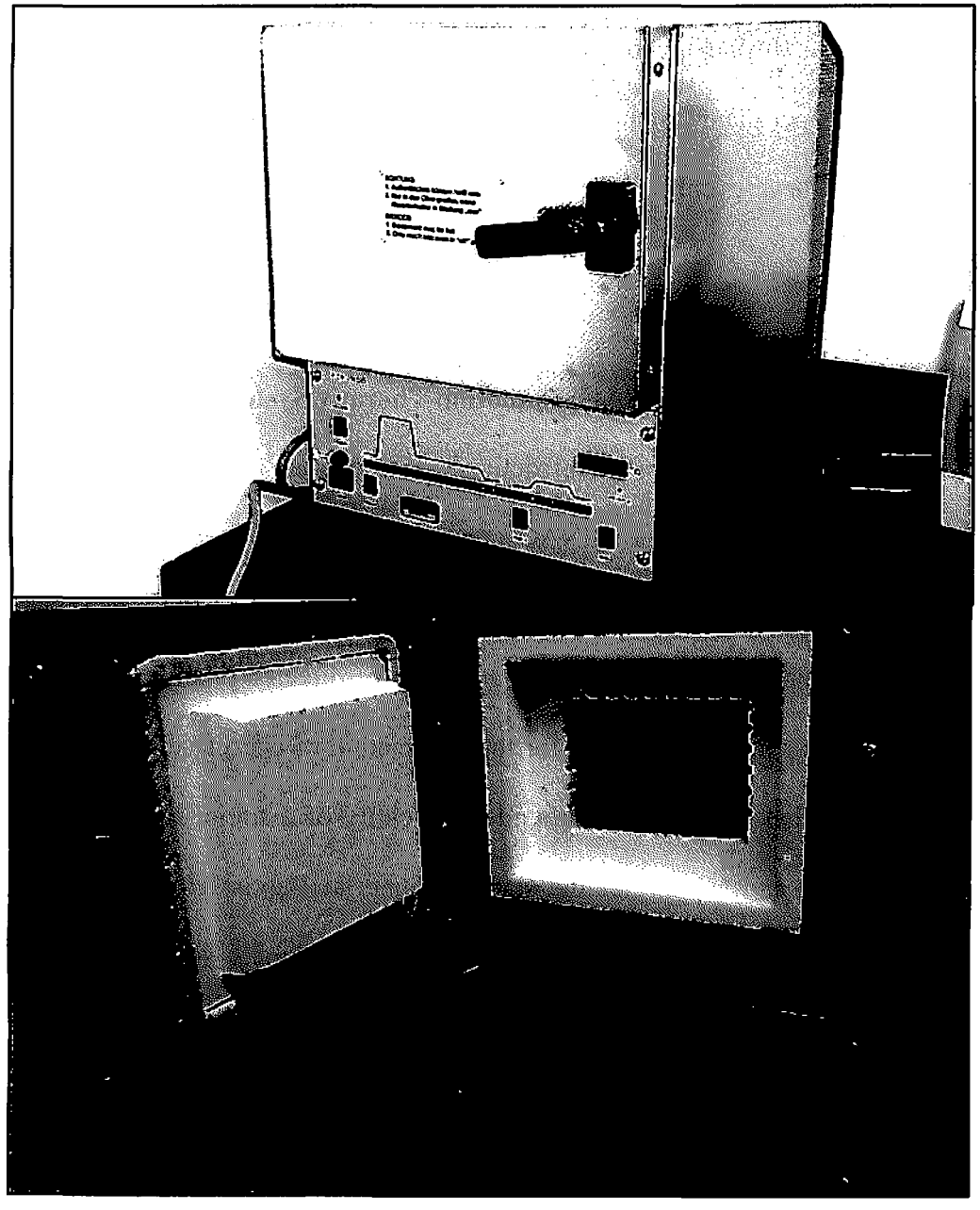

Figure 9. PTW-TLDO Annealing Oven

TLDs. For this study, program 1 was used with an initial heating temperature of 400 ^{o} C for approximately one hour, followed by 16 hours of annealing time at 80 ^{o} C to clear lower shallow traps. Inside the oven a shelf can hold 3 TLD plate holders, with a capacity of 42 TLDs per plate (Figure 3). The annealing oven also includes a built-in fan that distributes the heat evenly though the interior volume of the oven during the annealing process.

2.7 The Linear Accelerator (LINAC) Radiation Therapy System

A LINAC is an ionizing radiation delivery system that is used for the proper treatment of cancer patients. The LINAC can deliver 2 photon energies: 6 and 12 MegaVolts (MV), as well as five different electron energies (6, 9, 12, 15, and 18 MeV). By using these different forms of energy, radiation can be directed precisely towards the location of a benign or malignant tumor for the elimination of cancer cells, while at the same time ensuring that healthy cells around the vicinity of a tumor are not affected. With the cooperation and support of the staff members at Baptist Hospital Radiation Therapy Center, the LINAC located at this facility was the main source of radiation utilized for this study.

The LINAC utilized for this study is a CLINAC 2100c (Figure 10), manufactured by the Varian Corporation. The CLINAC 2100 produces ionizing radiation by the use of microwaves that accelerate electrons through an accelerator structure. The accelerated electrons are bent through magnets that redirect them to hit a target or metal plate that delivers high energy x-rays (Bremsstrahlung).

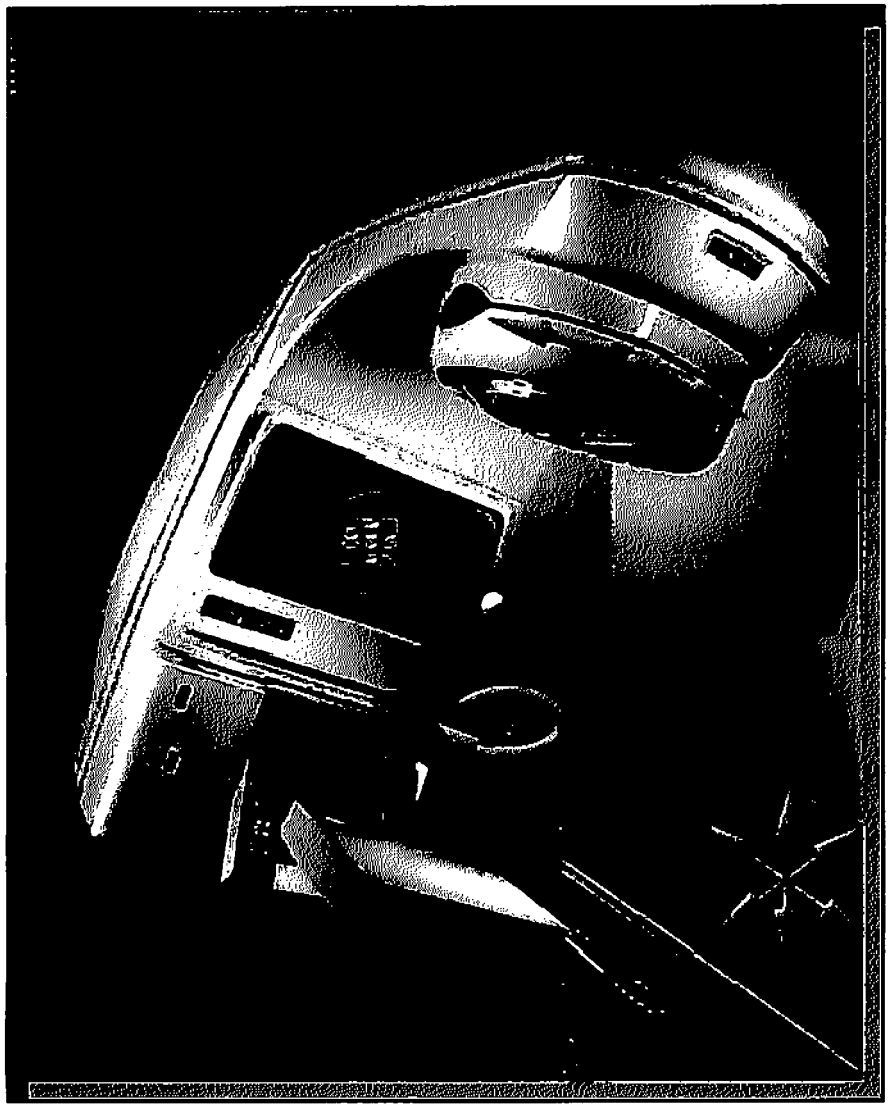

Figure 10. Varian CLINAC

Source: Baptist Cancer Treatment Center, Knoxville, TN

These high-energy photons are the treatment beam. The treatment beam can be shaped or filtered depending on the location and shape of the ROI. The shape of the beam can be attained by the use of multileaf collimators (MLC's). Small motors that arrange the collimators (MLC's) according to the shape of the treatment area drive one hundred and twenty tungsten collimators. Other forms of shaping the photon beams include the use of custom blocks made in-house. Custom blocks are used when the MLCs cannot assume the shape needed. Another form to modify the beam is through the use of wedges. These wedges are basically absorbing blocks that are put between the photon beam and the patient. The wedges are normally used to modify the dose distribution at the ROI, or isodose.

2.8 Computerized Tommography (CT) X-Ray System

Before any treatment is performed on a patient, an initial pre-scan with a Computerized Tommography (CT) X-Ray system is needed. The CT provides anatomical information about the patient and the treatment area. This information can then be transferred to the computerized system of the LINAC. During the imaging process, the CT scan will provide different electron densities (homogeneities or inhomegeneities) that the system will take into consideration when performing 3-D calculations in the pretreatment phase of the patient. An initial patient coordinate system is created during the CT scanning. By placing temporary or tattooed markers on the patient during the initial simulation and imaging, the patient can be repositioned on the LINAC system for future treatment planning and treatment delivery. The CT x-ray system used for this study is a General Electric "High Speed X1" Helical CT scanner.

Chapter 3

Experimental Methods

3.1 Calibration of TLD-100's (LiF:MG:Ti)

Before any data could be collected for this study, all 42 TLD-100's had to be calibrated properly. Knowing the exact dose produced by an ionizing source, proper calibration of TLDs can be performed. The purpose of calibration is to take into account any elements that may affect the TLD response and establish correction factors based on the known dose used. The main correction factors of interest are the element correction coefficient (ECC) and the reader correction factor (RCF).

3.1.1 NIST Calibrated Radiation source

The radioactive source utilized for calibration of the TLD-100's was a 1000 Ci Co-60 source, located at the U.S. Army Radiation Standards and Dosimetry Laboratory in Redstone Arsenal Alabama (Figure 11). The Co-60 was properly calibrated using the standards established by the National Institute of Standards and Technology (NIST) and it is traceable back to reference sources located at NIST. The NIST is considered to be the gold standard for calibration in the United States. This certifies a reliable and accurate exposure by the Co-60.

The Co-60 source is located in a high-energy photon room at the dosimetry center with all safety requirements for proper use of all the high-energy radiation sources located in this room. All handling of sources is performed remotely through a computerized system that, however, can be overridden for manual remote handling.

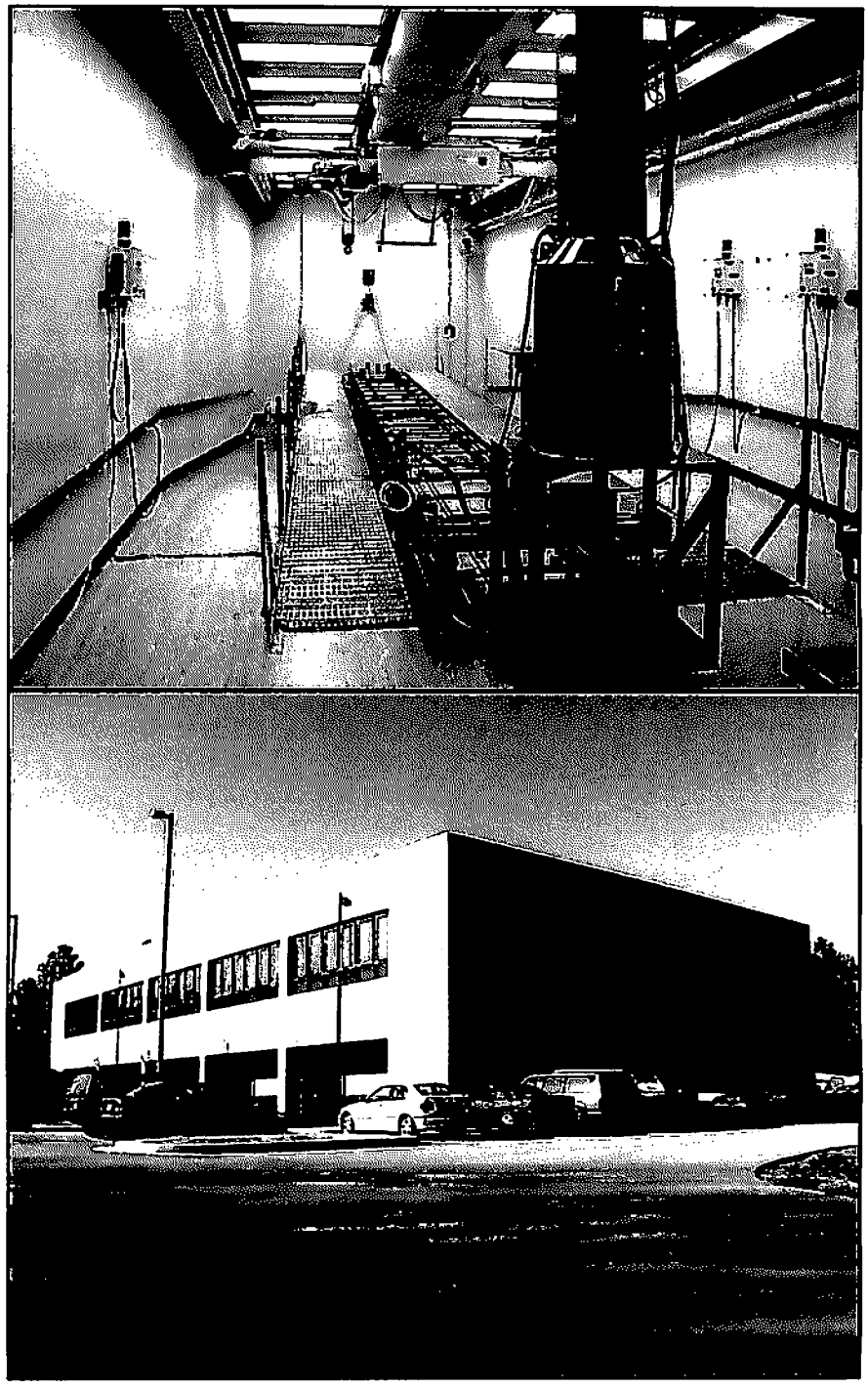

Figure 11. Co-60 and Cs-137 Sources. J.L Shepherd Model 81-22T

Source: U.S. Army Radiation Standards and Dosimetry Laboratory

The Co-60 source sits in a lead container (pig) with two additional Cs-137 sources that are brought up or down inside the lead container with a hydraulic arm system. When an object is to be exposed, a preset distance is set for the amount of radiation that it will be exposed to. Additionally, a set amount of time must also be determined in order for the object to receive the right amount of absorbed dose. Using the preset time and distance the object is then subjected to radiation. The object being subjected to radiation is placed at the preset distance by means of a rail system that is moved automatically by the computer system that controls the room. The Co-60 source is brought up with the hydraulic arm, and it is placed in front of a window. A lead shutter located in front of the window is moved away and the object is exposed until the preset time has ended. The shutter moves back in place closing the window and the source is brought down with the hydraulic arm.

3.1.2 Exposure of TLD-100's to NIST Co-60 Source

For calibration, the 42 TLDs used in this study were placed on a tissue equivalent plexiglass phantom within a 5 inch diameter circle. The phantom was positioned 1324 milimeters (mm) perpendicular to the beam and centered horizontally and vertically with the center beam in relation to the center of the 5 inch circle. A Helium-Neon (He-Ne) laser is used to determine the center of the beam before exposing an object. It is important to note that when an object is exposed within the 5 inches diameter circle, the dose distribution is uniform within the area of the circle (U.S. Dosimetry Center, 2003). The absorbed dose used to expose the TLDs was 175 R, delivered in 52.507 minutes. The conversion utilized to convert radiation exposure in air to rad or cGy is 0.879 rad per R. Therefore, the absorbed dose provided to each TLD was 153.85 rad or cGy.

3.1.3 Element Correction Coefficient (ECC)

Because all TLD-100's are not exactly the same, even within the batch in which they were produced, a correction factor must be introduced for every TLD element. A TLD can have some variation in materials composition and in size, compared to other TLDs. The response from the TLD will also be characteristic of that TLD and will be different from the response of other TLDs. Because of these differences, we must ensure the proper correction factor for each TLD element can be used for future exposure of that specific TLD. The correction factor utilized is called the Element Correction Coefficient (ECC) which is determined by the following equation:

$$ECC = \frac{<Q>}{Q_j} \tag{3.1}$$

where $<Q>$ is the average integrated charge in nano coulombs of all the calibrated TLDs, and Q_j is the total integrated charge for a specific TLD_j, also in nano coulombs

3.1.4 The Reader Correction Factor (RCF)

A correction factor must also be established for the type of reader used. Just as with the TLDs, every TLD reader has its own characteristics. TLD readers can vary from one to another, and therefore we must take into account the inherent characteristics of that TLD, i.e. if the system is automatic or manual, and the dependence on the inert gas utilized to reduce the noise of the PMT in the reader. The RCF is described mathematically as:

$$RCF = \frac{<Q>}{L} \quad , \tag{3.2}$$

where $<Q>$ is the average charge value in nanocoulombs of all the calibrated TLDs and L is the exposure given to the TLDs that are being calibrated.

3.1.5 Dose Determination for each TLD-100 Chip

If we rearrange equation 3.1 with respect to <Q> and Equation 3.2 with respect to L we obtain,

$$<Q> = ECC_j * Q_j \tag{3.3}$$

$$L = \frac{<Q>}{RCF}, \tag{3.4}$$

Replacing <Q> in equation 3.4 with the value of <Q> from 3.3, then

$$L_j = \frac{ECC_j * Q_j}{RCF}, \tag{3.5}$$

where L_j is the unit dose value for TLD element j. A relationship must now be established between the actual exposure in R and the unit dose value in each TLD element. The relationship can be expressed by K, which becomes the conversion factor from R to rad, when L_j is given in rad.

$$K = \frac{L_j}{R} \tag{3.6}$$

Adding this conversion factor into Equation 3.5, we get that

$$L_j = \frac{ECC_j * Q_j}{RCF * K} \tag{3.7}$$

For the LINAC system, the K conversion ratio is 1 since the LINAC is set to produce 1 cGy per machine click. When the LINAC is in use, the machine actually produces a click sound for each 1 cGy of exposure. Since K is equal to 1, the actual dose D_j to a TLD element j is then:

$$D_j = \frac{ECC_j * Q_j}{RCF} \tag{3.8}$$

After exposure of all 42 TLDs, a workspace file in WinRems© was created before reading the TLDs with the Harshaw 3500 TLD Reader.

3.1.6. Workspace File Setup

The following parameters were set for the Time Temperature Profile (TTP) and the acquisition parameters:

3.1.6.1 Time Temperature Profile (TTP)

Regions of Interest(ROI): A total region of 200 channels was set, divided in four regions of interest:

ROI 1 = 0-50 ROI 2 = 50-100

ROI 3 = 100-150 ROI 4 = 150-200

Preheat Temperature: 50°C

Acquisition Temperature Rate: 10°C/sec reaching maximum temperature of 300° C.

Anneal Temperature: 300° C

RCF and Background: Not set.

3.1.6.2 Acquisition Setup

For the acquisition setup, we accepted the software default values recommended for this study with the exception of the ECC and the RCF factor that were not applied. PMT noise and light reference were left at default values of occurrence every 10 TLDs.

3.1.7 TLD Calibration Reading

All TLD 100's were read within 24 hours after exposure to take into account possible fading. Nitrogen flowed through the reader 30 minutes prior to initial readings of the TLDs. All 37 TLD-100 were then read and the numerical output of the integrated charge (nC) for all the TLDs was exported to a spreadsheet. The spreadsheet calculations of the RCF and the ECC's for each TLD are shown in Table 3.1.

3.2 Linear Dose Response

Prior to exposing the TLD-100 within the anthropomorphic phantom, 25 of the 37 calibrated TLDs were exposed to different exposure levels to determine the linear response to ionizing radiation imparted by the LINAC system utilized for this study. The 25 TLDs were divided into five groups and each group was exposed to different radiation exposure levels. The range of radiation exposure was from 5 cGy to 1000 cGy. Every TLD was placed at exactly 100 cm from the source to an equivalent skin tissue that was

Table 3.1 Calibration of TLD-100's (LiF:Mg:Ti)

TLD	Q_j		<Q>	ECC_j	Dose NIST source	RCF (nC/cGy)	D_j(cGy) $(ECC_j*Q_j)/(RCF*K)$
	NC Gross	nC Net *		$<Q>/Q_j$	(D)cGy	<Q>/D	
1	23313.59	23313.44	22617.41	0.97	153.85	147.01	153.85
2	24126.72	24126.57	22617.41	0.94	153.85	147.01	153.85
3	24732.78	24732.63	22617.41	0.91	153.85	147.01	153.85
4	24193.93	24193.79	22617.41	0.93	153.85	147.01	153.85
5	21913.62	21913.47	22617.41	1.03	153.85	147.01	153.85
6	21078.48	21078.33	22617.41	1.07	153.85	147.01	153.85
7	23094.99	23094.84	22617.41	0.98	153.85	147.01	153.85
8	25159.20	25159.06	22617.41	0.90	153.85	147.01	153.85
9	24544.27	24544.12	22617.41	0.92	153.85	147.01	153.85
10	22528.62	22528.47	22617.41	1.00	153.85	147.01	153.85
11	24484.86	24484.71	22617.41	0.92	153.85	147.01	153.85
12	23238.89	23238.74	22617.41	0.97	153.85	147.01	153.85
13	24466.65	24466.50	22617.41	0.92	153.85	147.01	153.85
14	24630.92	24630.78	22617.41	0.92	153.85	147.01	153.85
15	22775.03	22774.88	22617.41	0.99	153.85	147.01	153.85
16	23618.64	23618.50	22617.41	0.96	153.85	147.01	153.85
17	23659.34	23659.19	22617.41	0.96	153.85	147.01	153.85
18	23164.90	23164.75	22617.41	0.98	153.85	147.01	153.85
19	22773.98	22773.83	22617.41	0.99	153.85	147.01	153.85
20	23954.17	23954.02	22617.41	0.94	153.85	147.01	153.85
21	23483.07	23482.93	22617.41	0.96	153.85	147.01	153.85
22	21949.70	21949.56	22617.41	1.03	153.85	147.01	153.85
23	20981.74	20981.59	22617.41	1.08	153.85	147.01	153.85
24	22769.76	22769.61	22617.41	0.99	153.85	147.01	153.85
25	24847.60	24847.46	22617.41	0.91	153.85	147.01	153.85
26	22322.46	22322.31	22617.41	1.01	153.85	147.01	153.85
27	22124.52	22124.37	22617.41	1.02	153.85	147.01	153.85
28	20402.31	20402.17	22617.41	1.11	153.85	147.01	153.85
29	21398.02	21397.87	22617.41	1.06	153.85	147.01	153.85
30	22059.55	22059.40	22617.41	1.03	153.85	147.01	153.85
31	22682.79	22682.64	22617.41	1.00	153.85	147.01	153.85
32	18914.73	18914.58	22617.41	1.20	153.85	147.01	153.85
33	22464.30	22464.15	22617.41	1.01	153.85	147.01	153.85
34	18847.80	18847.66	22617.41	1.20	153.85	147.01	153.85
35	21212.39	21212.24	22617.41	1.07	153.85	147.01	153.85
36	19990.58	19990.43	22617.41	1.13	153.85	147.01	153.85
37	18944.79	18944.64	22617.41	1.19	153.85	147.01	153.85

* Background: 0.148 nC

previously placed on top of the TLDs. The Multileaf collimators (MLC's) were placed in a 10 x 10 square arrangement. To determine the linearity of the data, the Statistical Analysis Software (SAS Institute, 1999) was utilized to create a simple linear regression model.

The equation that represents a simple regression model can be described as:

$$Yi = \beta_o + \beta_1 * X + \varepsilon \qquad (3.9)$$

Where Yi is the response variable, β_o and β_1 are estimated parameters for the line intercept and the slope value respectively for the linear model. X is the independent variable and ε is the random error term or residual (Neter *et al*, 1996). Table 3.2 show the data used to determine the linearity of the TLDs.

The data include the integrated charge (nC) provided by the TLD reader, the net integrated charge after background removal (0.49867 nC), different levels of exposure from the LINAC systems as well as the measured dose at each set LINAC dose.

3.3 Patient Treatment planning of the ART Phantom

The ART Phantom was initially placed on the table of the CT scanner system and aligned properly for initial CT scanning. Temporary markers were placed on the hips and the stomach of the phantom with the help of He-Ne lasers that marked the phantom in the axial and coronal axis. After the coordinate system was established for the phantom, a CT pre-scan was conducted to determine anatomical characteristics of the phantom, as well as to determine the mock location of the ROI in the cervix area of the phantom.

Table 3.2 Data Used to Check Linearity

TLD	Integrated Charge(nC)	Net Integrated Charge (nC)*	LINAC Dose (cGy)	Measured TLD Dose (cGy)
1	871.80	871.30	5	5.75
2	945.02	944.52	5	6.02
3	1076.32	1075.82	5	6.69
4	1119.25	1118.75	5	7.11
5	8284.38	8283.88	50	58.16
6	11072.08	11071.58	50	80.81
7	11177.43	11176.93	50	74.46
8	11476.76	11476.26	50	70.18
9	17177.45	17176.95	100	107.67
10	22632.85	22632.35	100	154.56
11	23218.74	23218.24	100	145.89
12	23962.67	23962.18	100	158.64
13	32957.53	32957.03	200	207.24
14	33037.48	33036.99	200	206.36
15	33450.34	33449.85	200	225.96
16	34462.64	34462.14	200	224.48
17	89255.61	89255.11	500	580.40
18	97239.19	97238.69	500	645.81
19	128758.23	128757.73	500	869.83
20	137629.45	137628.95	500	883.95
21	140071.88	140071.38	500	917.68
22	197900.95	197900.45	1000	1387.13
23	209517.34	209516.85	1000	1536.30
24	288022.25	288021.75	1000	1946.10
25	291942.25	291941.75	1000	1807.63

Background: 0.49867 nC

Figure 12 shows how the TPS established the location of the ROI for this study. The computer interface of the TPS also provides other forms of data that the oncologist or medical physicist can utilize for the pretreatment phase of a patient. All the data for the ART phantom information was transferred to this TPS for additional treatment planning and future dose irradiation of the phantom by the LINAC system.

In Figure 12, the top image shows an AP view of the ART phantom with the location of the mock tumor (red mass). The TPS is set on the x and y coordinate system on this view and it is aligned the same way from an axial position (Lower image). The square surrounding the mock tumor is the radiation field delimited by the MLC's.

3.4 TLD Setup in the ANDRO Anthropomorphic Phantom

Thirty seven TLD-100's initially annealed at 300°C were placed in the ART Phantom in slices 28 thru 33. For the placement of a TLD, a plug was removed from the slice. The plug was then cut in the middle at exactly the thickness of the TLD. The bottom portion of the plug was placed back in its original position. The TLD was placed next with the top portion of the plug above the TLD.

Appendix I shows the location of each TLD placed in the ART phantom. The intention was to get as many TLDs as possible sufficiently close to the isocenter located in slice 30. TLDs were inserted in this slice and in slices below and above slice 30.

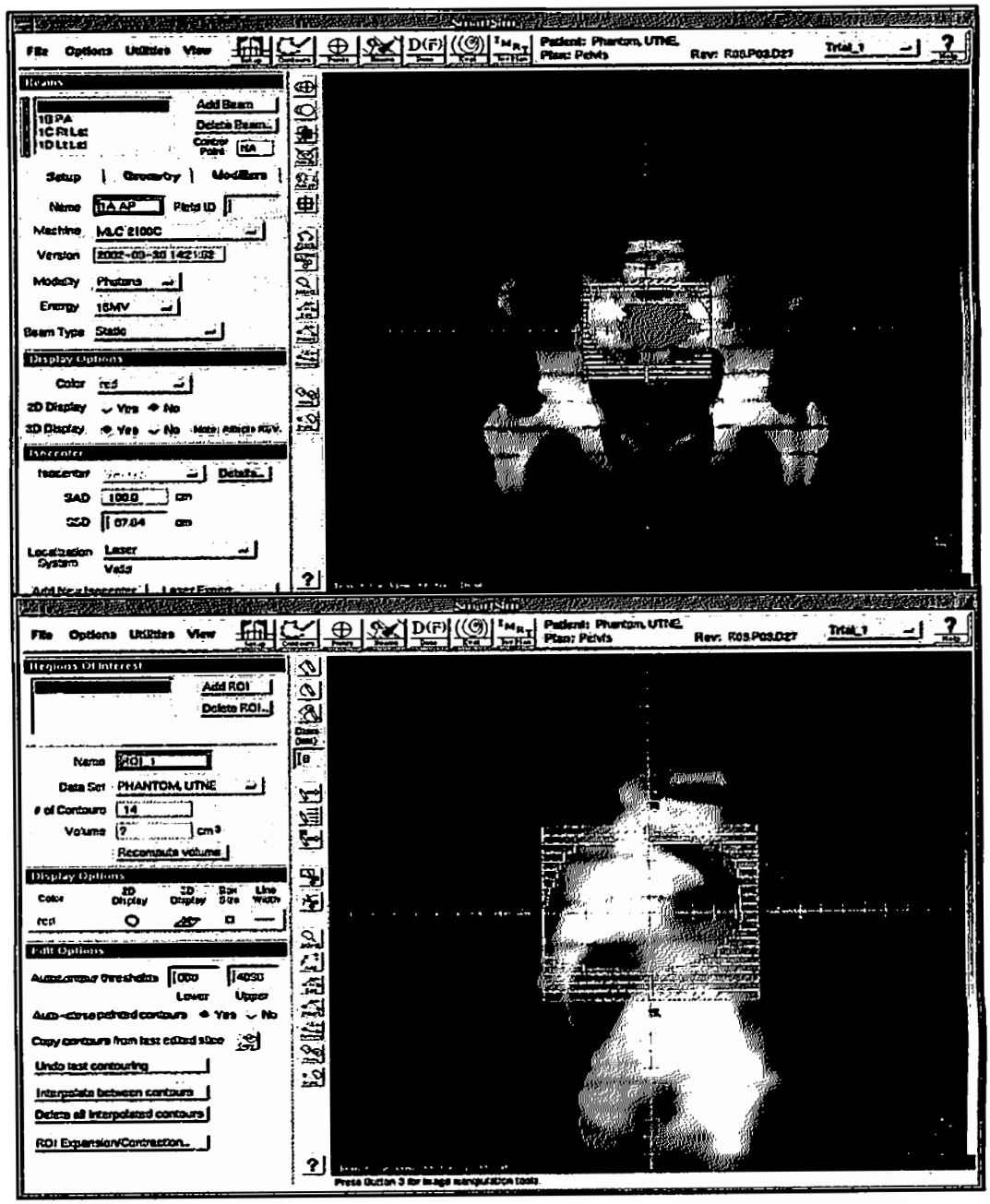

Figure 12. 3D dimensional view of Mock Tumor on the ART anthropomorphic Phantom

Source: Baptist Cancer Therapy Center, Knoxville, TN

Figure 13 is a cross-sectional image created by the CT scanner at isocenter (Slice 30). The colored contoured lines represent the gradient dose calculated by the 3 dimensional TPS. You will also see in this Figure a grid system on the ART phantom. The grid points are plugs that can be removed from the ART phantom and costumed to accommodate a specific type of TLD. Each TLD was placed in the middle of the transverse plug.

3.5 ART Phantom setup and Exposure

After proper placement of the TLDs, the ART phantom was taken once again to Baptist Cancer Treatment Center, and it was placed in a supine position on the LINAC table. In order to align the ART phantom correctly, the coordinate system previously established in the pretreatment planning phase was used. Using this information and with the help of positional lasers the ART phantom was aligned correctly on the LINAC table, to ensure proper exposure in the ROI. The gantry of the LINAC system was positioned at 100 cm Source-Axis Distance (SAD) to isocenter of the ART phantom and the MLC's were set in a 10 x 10 square geometry. After proper setup, the ART Phantom was exposed to 180 cGy to isocenter.

The TLDs were removed from the ART phantom and read by the TLD reader the next day. The absorbed dose was established for each TLD using the RCF and ECC's previously established during the calibration period.

The difference between the calculated dose and the measured dose is determined using the normalized dose difference (NDD). The NDD method is used extensively in quality control and quality assurance in radiation therapy.

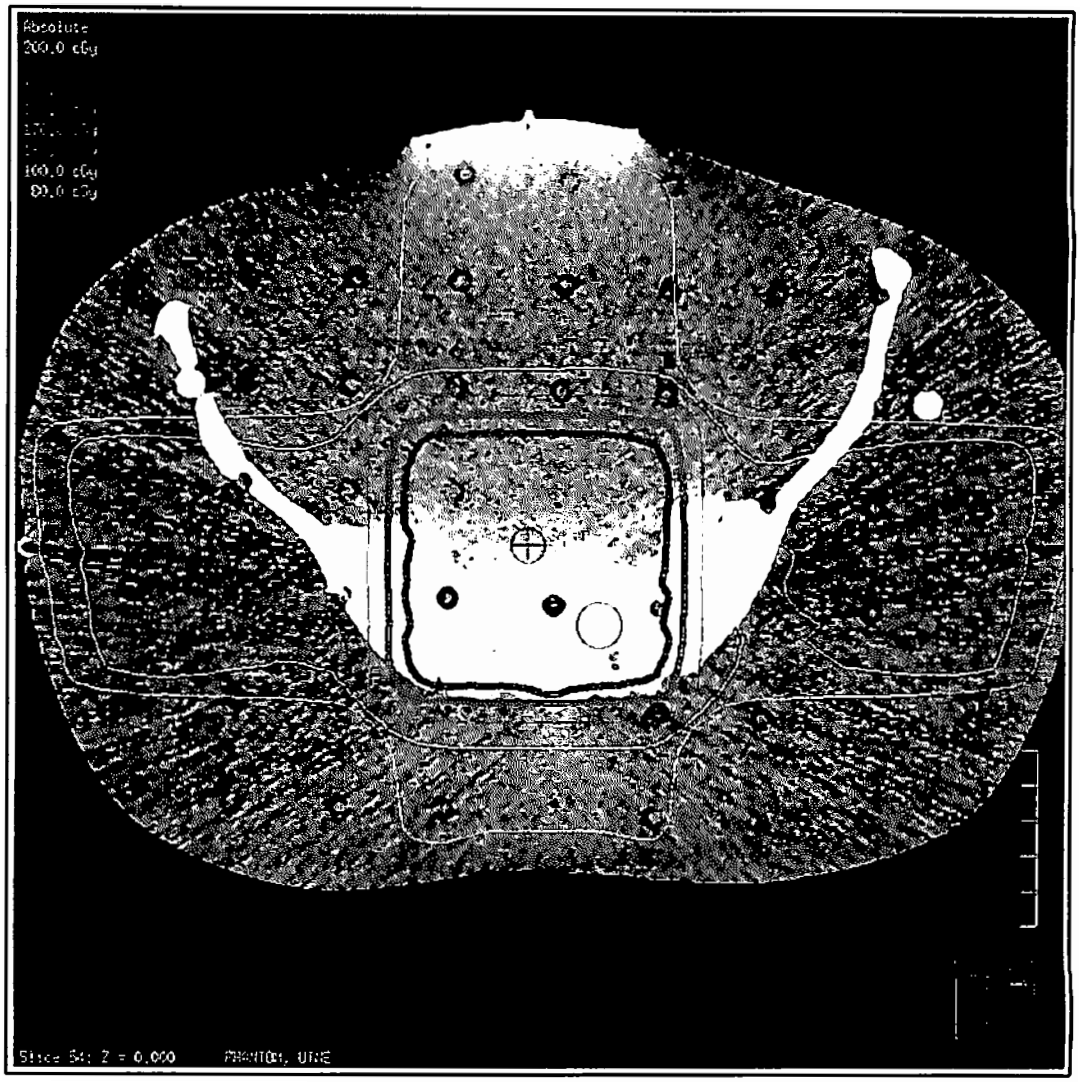

Figure 13: CT Crosssectional view of the ART Phantom and diagram of TLD location

Source: CT Image from Baptist Cancer Treatment Center

The NDD at a point (Dunscombe *et al, 1995*) is defined as:

$$NDD = (\text{Calculated Dose} - \text{Measured Dose})/\text{Nominal isocenter Dose} \quad (3.10)$$

where the nominal isocenter dose is the absorbed dose calculated for the isocenter on the basis of 100 monitor units (MU) per beam (Dunscombe *et al, 1995*). By conveying the NDD as a percentage, NDD values provided can be compared to the acceptance criterion proposed by Van Dyk *et al* (1993). The measured absorbed dose for each TLD, the calculated dose and the NDD are shown in table 3.3.

3.6 Comparison of Dose Response of the Panasonic TLD system and TLD-100

In addition to the main study, a comparison of dose response by the TLD-100's and the Panasonic TLD system was performed. The intent is to verify the reliability of TLD 100's used in this study.

Twenty five Panasonic TLDs and 26 TLD-100's were exposed by the LINAC System with a pre-established dose of 100 cGy with the multi-leaf collimators set at 10 x 10 cm. Before the exposure of the TLD-100's the RCF were re-established once again based on an exposure to the 100 cGys provided by the LINAC system. The original ECC from the initial calibration were kept.

Both TLD systems were set in batches on top of a solid tissue equivalent phantom, with the latter placed on top of the patient's table. The tube was placed stationary vertical over the TLD systems with a Skin to Source Distance (SSD) of 100

Table 3.3 Doses to TLD-100's in the ART Anthropomorphic Phantom

				TLD 100 (LiF:mg:Ti) in Phantom			TPS** Dose	
TLD	Phantom Slice No.	ECC_j <Q>/Q_j	RCF <Q>/D	nC Gross	nC Net	Dose (cGy)	(cGy)	NDD%
1	33	0.97	147.01	445.11	444.93	2.94	2.18	0.42%
2	33	0.94	147.01	419.23	419.05	2.67	2.11	0.31%
3	33	0.91	147.01	459.70	459.52	2.86	1.78	0.60%
4	33	0.93	147.01	399.86	399.68	2.54	2.20	0.19%
5	33	1.03	147.01	432.46	432.27	3.03	2.28	0.42%
6	33	1.07	147.01	379.34	379.15	2.77	1.88	0.49%
7	33	0.98	147.01	349.40	349.22	2.33	1.48	0.47%
8	32	0.90	147.01	1329.23	1329.05	8.13	11.05	-1.62%
9	32	0.92	147.01	1300.65	1300.47	8.15	12.85	-2.61%
10	32	1.00	147.01	1108.80	1108.62	7.57	8.48	-0.51%
11	32	0.92	147.01	827.76	827.58	5.20	5.72	-0.29%
12	32	0.97	147.01	929.12	928.94	6.15	8.85	-1.50%
13	32	0.92	147.01	1107.17	1106.99	6.96	9.58	-1.46%
14	32	0.92	147.01	809.44	809.26	5.05	6.28	-0.68%
15	32	0.99	147.01	774.06	773.88	5.23	3.80	0.79%
16	32	0.96	147.01	694.39	694.21	4.52	3.18	0.75%
17	31	0.96	147.01	20988.75	20988.57	136.48	159.47	-12.77%
18	31	0.98	147.01	21801.79	21801.61	144.80	172.40	-15.34%
19	31	0.99	147.01	12124.03	12123.85	81.90	92.20	-5.72%
20	31	0.94	147.01	14151.77	14151.59	90.89	128.90	-21.12%
21	31	0.96	147.01	21805.41	21805.23	142.86	146.20	-1.86%
22	31	1.03	147.01	17717.73	17717.55	124.19	138.90	-8.17%
23	30	1.08	147.01	24647.71	24647.52	180.73	184.90	-2.32%
24	30	0.99	147.01	16398.13	16397.94	110.80	128.50	-9.83%
25	30	0.91	147.01	26306.96	26306.78	162.88	182.80	-11.06%
26	30	1.01	147.01	24318.75	24318.57	167.61	177.90	-5.72%
27	30	1.02	147.01	24889.24	24889.06	173.07	184.70	-6.46%
28	30	1.11	147.01	11085.74	11085.56	83.59	88.67	-2.82%
29	30	1.06	147.01	12349.49	12349.31	88.79	87.40	0.77%
30	29	1.03	147.01	25809.80	25809.62	180.00	180.80	-0.44%
31	29	1.00	147.01	17021.11	17020.93	115.45	134.10	-10.36%
32	29	1.20	147.01	21930.87	21930.69	178.38	180.50	-1.18%
33	29	1.01	147.01	26234.92	26234.74	179.67	173.00	3.71%
34	29	1.20	147.01	23218.44	23218.26	189.52	181.10	4.68%
35	28	1.07	147.01	3380.25	3380.07	24.52	29.13	-2.56%
36	28	1.13	147.01	1492.39	1492.21	11.48	16.38	-2.72%
37	28	1.19	147.01	1358.39	1358.21	11.03	14.50	-1.93%

* Background: 0.181 nC

** Treatment Plannng system (TPS). Calculated Dose

The SSD was actually set to a skin tissue equivalent material on top of the TLD systems. The dose response for both TLD systems is presented in Table 3.4.

Table 3.4 Dose Comparison between TLD-100 and Panasonic TLDs

TLD-100 (Li:Mg:Ti)			Panasonic TLD		
Dose (cGy)	Difference	Percent difference	Dose (cGy)	Difference	Percent difference
95.118	-4.882	-4.88%	99.522	-0.478	-0.48%
105.717	5.717	5.72%	94.842	-5.158	-5.16%
111.065	11.065	11.07%	91.255	-8.745	-8.75%
96.223	-3.777	-3.78%	92.137	-7.863	-7.86%
98.868	-1.132	-1.13%	102.665	2.665	2.67%
97.247	-2.753	-2.75%	103.824	3.824	3.82%
98.943	-1.057	-1.06%	101.777	1.777	1.78%
97.589	-2.411	-2.41%	101.016	1.016	1.02%
96.801	-3.199	-3.20%	104.314	4.314	4.31%
98.886	-1.114	-1.11%	104.416	4.416	4.42%
98.972	-1.028	-1.03%	99.155	-0.845	-0.84%
97.637	-2.363	-2.36%	99.155	-0.845	-0.84%
99.486	-0.514	-0.51%	97.594	-2.406	-2.41%
97.739	-2.261	-2.26%	97.594	-2.406	-2.41%
99.949	-0.051	-0.05%	100.15	0.15	0.15%
102.001	2.001	2.00%	100.15	0.15	0.15%
100.967	0.967	0.97%	99.831	-0.169	-0.17%
99.245	-0.755	-0.76%	99.831	-0.169	-0.17%
106.303	6.303	6.30%	101.835	1.835	1.83%
109.825	9.825	9.83%	101.835	1.835	1.83%
107.370	7.370	7.37%	92.613	-7.387	-7.39%
104.167	4.167	4.17%	92.613	-7.387	-7.39%
105.744	5.744	5.74%	110.113	10.113	10.11%
108.501	8.501	8.50%	110.113	10.113	10.11%
113.683	13.683	13.68%	105.636	5.636	5.64%

Chapter 4

Data Analysis

4.1. Determination of linearity

Utilizing the set dose and the response dose of the TLD, the required SAS (SAS Institute, 1999) code (Appendix II), was created to perform the regression analysis. SAS codes for this regression analysis can be found in Appendix II. Using the SAS code (SAS Institute, 1999) we created a simple linear regression analysis and also produced a scatter plot (Figure 14) with the estimated linear regression model. In addition, a plot of the residuals versus the set LINAC dose was also created in order to look at the variation of the estimated doses from the set dose, as well as possible outliers in the data (Figure 15).
The linear model produced for the data set is expressed as:

$$Y_i = -40.78014 + 1.68363\,X$$

Figure 14 shows that data at lower values seem to fit closer to the linear regression function. However, for values above 200 cGys the data points spread out showing larger variations from the regression model.

If we look at the plot of residual values vs predicted values (Figure 15), it is also evident that residuals at higher doses show larger differences or variance from measured data, almost four times the difference values below 200 cGys. The strength of the linear relationship between the set dose and the measured dose can be determined by using the determination coefficient (r^2). Values of r^2 close to 1 or -1 indicate a strong relationship

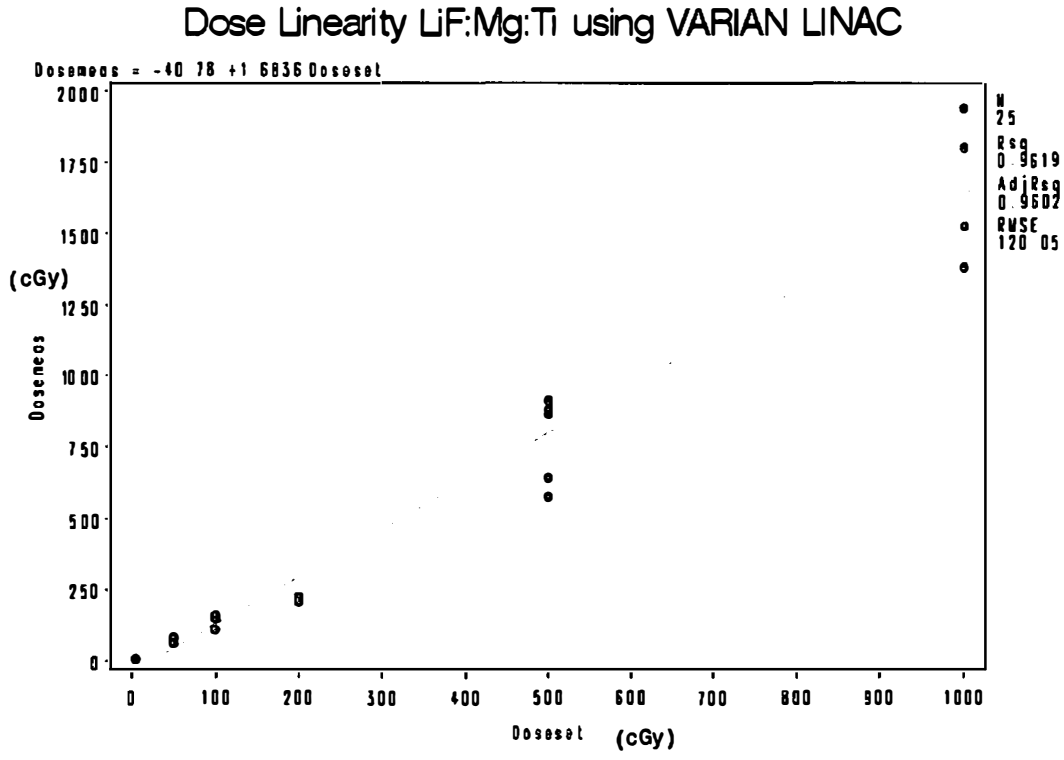

Figure 14. Dose Response Linearity of TLD-100

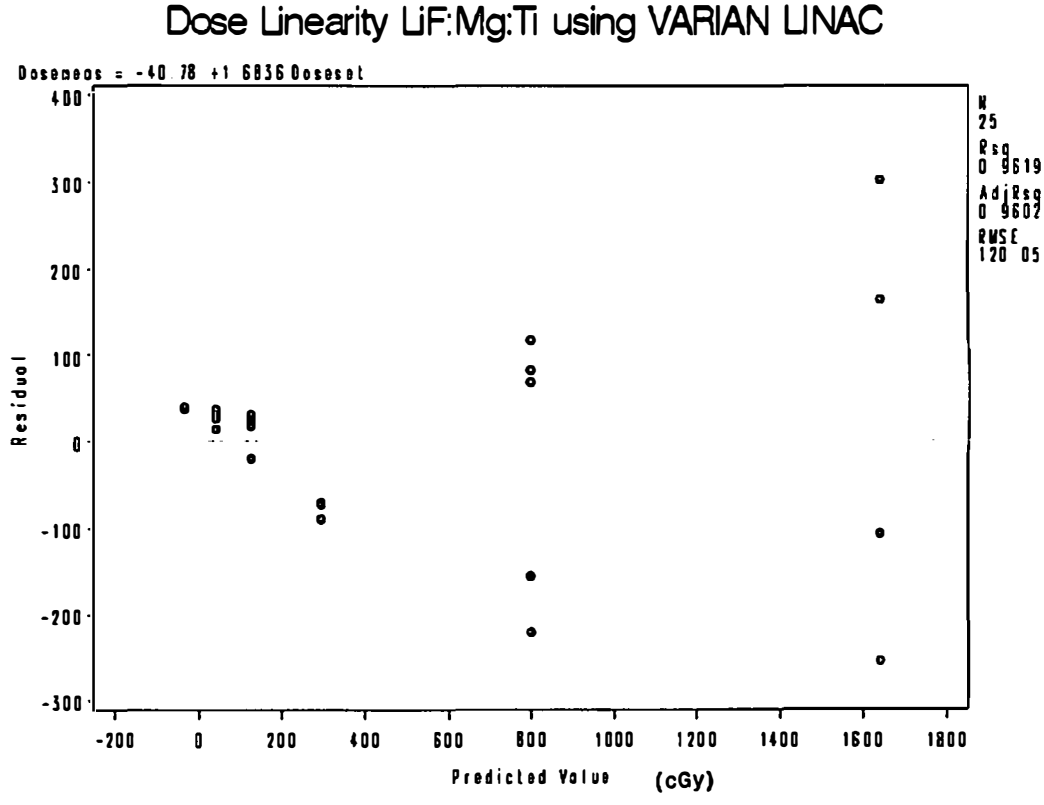

Figure 15. Dose Residual values Vs. Predicted values

between the two variables and a strong fit of the values to the linear regression function. The r^2 value for this model is 0.9619 indicating the strength between these two values even though there are large variances at higher dose energies. Based on this analysis, the data produced by the TLD reader do not appear linear for values above 200 cGy, which is possibly caused by linearity fluctuations of the TLD reader (Paragraph 2.5.1) or the actual TLD elements.

For this study, we did not use doses above 200 cGy. Therefore, concerns for high variances in the dose response of the TLD-100's are minimal.

4.2 Comparison Between Treatment Planning (TPS) System and TLD-100

Several factors must be taken into consideration when trying to verify the dose to a specific point in the ART phantom. One factor is the different densities in different tissue equivalent materials in the phantom; another one is the potential existence of inhomogeneities in these different materials. Another issue of concern in this study was the process of verifying the correct location of the TLD's in the ART phantom with the use of the TPS. Each slice of the ART phantom is exactly 2.5 cm. This thickness is not equivalent to the different slices created initially during the CT pre-scan phase. The CT produces radiological images every other 2.4 cm above and below the isocenter. Because of this difference in thickness there is a possibility that the values at a certain point using the TPS might be below or above the location of a specific TLD. At isocenter the location for TLD's will be correct but for TLD's below and above there will be variations in the actual location of the TLD. The large differences between the calculated dose

expressed by the TPS and the measured dose of the TLD's might be explained by this difference in slice thickness.

With these issues in mind, initial observations of differences at isocenter (Slice 30) were reviewed. TLD 23 located exactly at the isocenter showed an NDD % of 2.32. Other TLD's around TLD 23 followed the requirements met by TLD 23. However a few TLD's exceeded the required percentage of 5 percent. This percent increase above the required value can be attributed to some of the issues described above. TLD 25 is located in bone and shows a percent difference of 11.06 %. Other differences (TLD 26, 27) exceeding the standards can be attributed to inhomogeneities or proximity to inhomogeneities present in the tissue equivalent material of the ART phantom.

TLD 30, located exactly 2.5 cm above isocenter (Slice 29) showed that placement at this distance gave quite accurate results with a percent difference of only 0.44 % between the measured and calculated dose. All other TLD's in slice 29 of the ART phantom were below the required 5%, with the exception of the location where TLD 31 is sited. This TLD is shown to be located in the soft tissue region of the phantom. There seems to be no large amount of inhomogeneity but, as mentioned previously, the location of the TLD is not exactly at the location that the TPS is reading. These show that within a few millimeters, the doses calculated by the TPS at two different points can show large differences because of the dose gradient that is calculated by the TPS.

For TLD's that are located farther away from the isocenter both the calculated dose and the measured dose decrease with increased distance. In radiation therapy treatment this is exactly what is needed. The intention is to deliver the full dose to isocenter where the tumor is located and ensure that healthy tissue around the tumor gets minimal

exposure (Khan, 2003). This provides the healthy tissue with the chance to recover from the dose exposure imparted, while at the same time killing the cancer cells.

In Fig 16 a multiple column graph showing the differences in measured dose and calculated dose is presented. No apparent differences between doses can be appreciated at a glance, except around TLD 20 where a large difference is shown. Further analysis of the data (Fig 17) shows that of the 37 TLD's utilized, 27 % exceeded the dose difference of 5% between the calculated and the measured dose. Additionally 13.51 % exceeded the NDD of 10% for this difference. These differences can be observed for each TLD, with the larger difference occurring at TLD 20, located in slice 31, and placed on the lower end of the vertebrate of the ART phantom. Further analysis also shows that there is a trend for TLD exceeding the established 5% to be located close to areas which are within or close to inhomogeneities. On the hand, TLD's farther away from isocenter show values that are below the established limit.

4.3 Paired Data Analysis between TLD-100 and the TPS

In statistical analysis there are several methods used to compare two sets of data. Before we compare the two data sets it is important to understand that when comparing the data points, they are both exposed to the same dose at a certain location. So for every specific TLD location, we are comparing it to the calculated dose by the TPS at that location.

Before considering which method is the most appropriate for this study, the normality of the two data sets must be established, as well as the normality for the

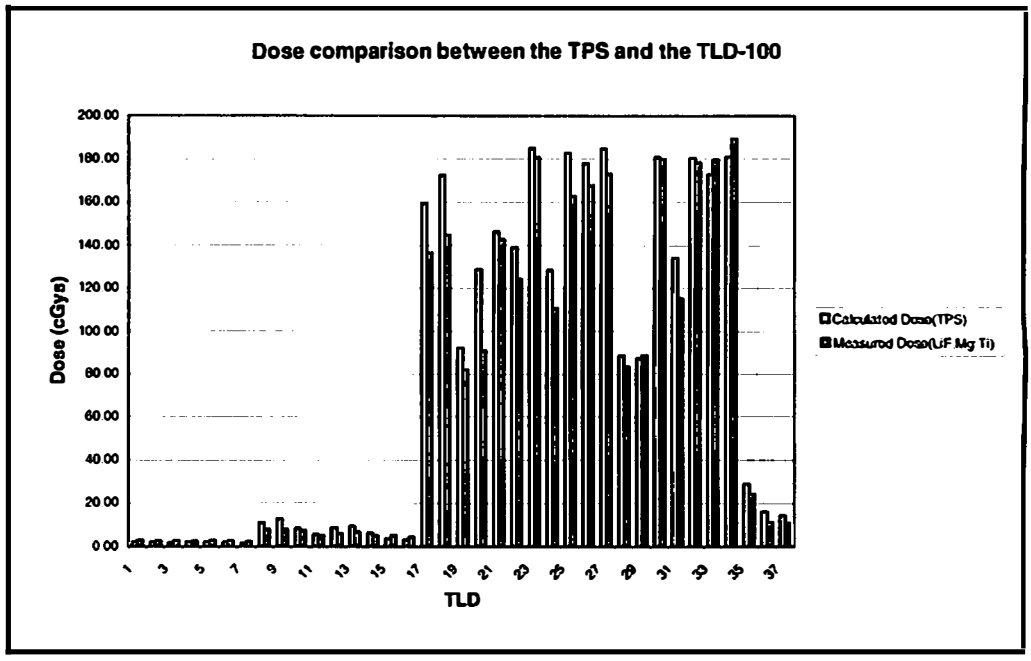

Figure 16. Dose Comparison between the TPS and TLD-100

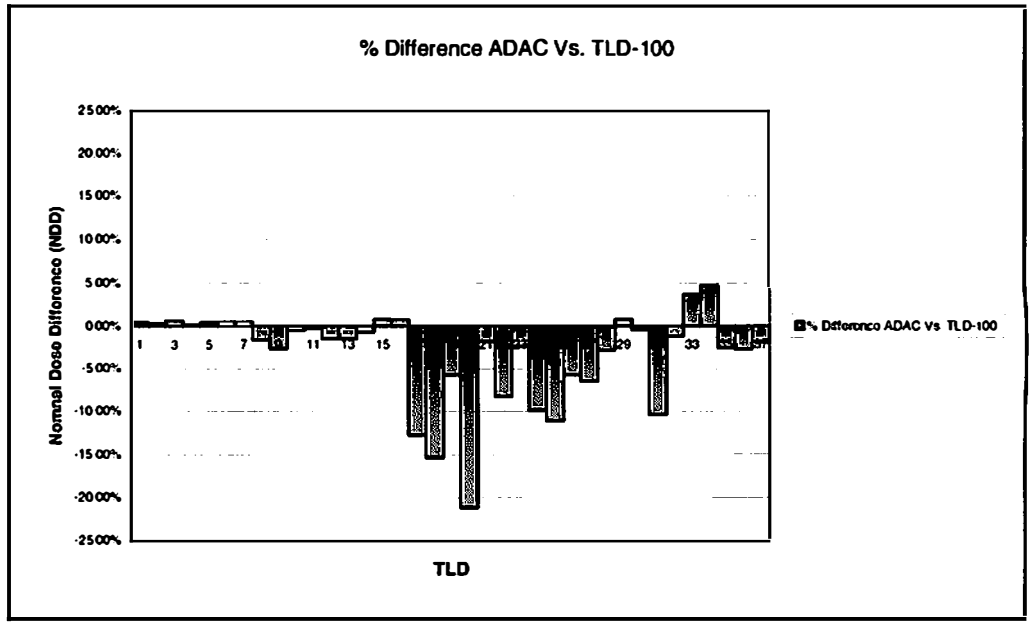

Figure 17. Percent Difference between measured Dose anc Calculated Dose

differences between the data from the TLD-100 and the TPS. In addition other tests can be performed that will complement the analysis of the paired data, i.e. the difference in means, difference in variances, etc. This will give us a better perspective on how equal or unequal the data sets might be.

The statistical software utilized for the data analysis once again is SAS (Appendix II). Before looking at any numbers, frequency histograms for both the TLD-100's as well as for the difference of the two (Figure 18 and 19.) were created. When looking at the frequency histograms for the measured dose of the TLD- 100 and the calculated dose of the TPS, we can observe that their distributions are almost identical, but they do not have normality. Because of non-normality of the raw data of the TPS and the TLD-100 we instead use the difference of the data sets, which does present a normal distribution of the data, though the data are skewed to the left.

The normality of the data that are presented in blue is determined by SAS using the probability distribution function:

$$f(y) = \frac{1}{\sqrt{2\pi}\sigma} e^{(y-\mu)^2/2\sigma^2} \quad , \qquad (4.2)$$

where μ is the population mean, and σ is the standard deviation of the data.

Observe from Figure 19 that approximately 60 to 75 percent of the differences under the bell shaped curve are small between TLD 100 and the TPS. SAS also provide in the output basic statistical data of the moments and the variance of the data.

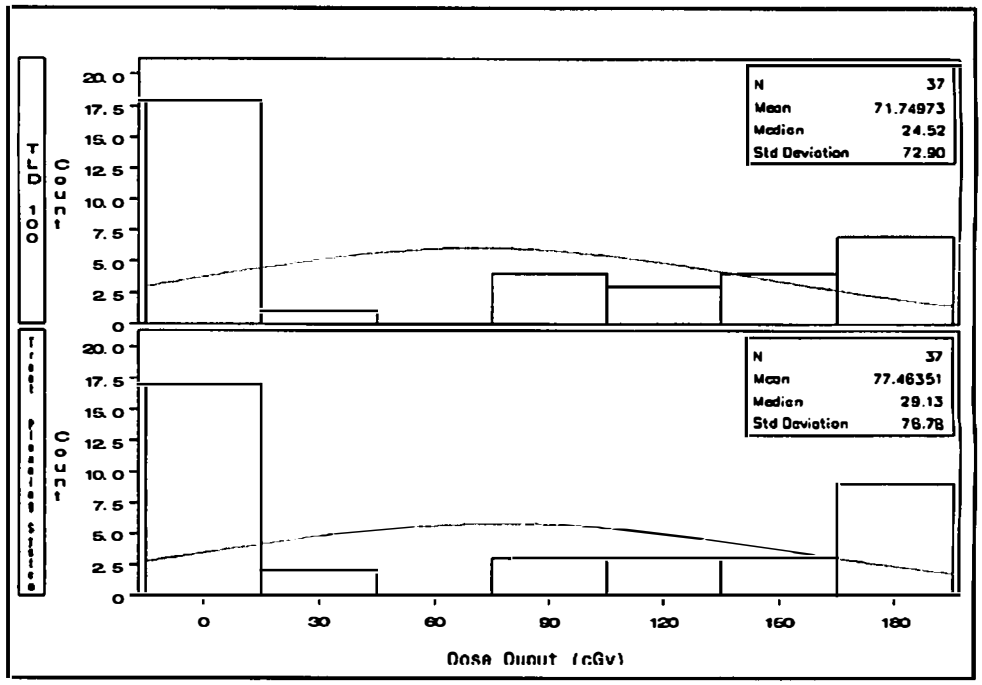

Figure 18. Comparison of Data Distribution between TLD-100 and the TPS

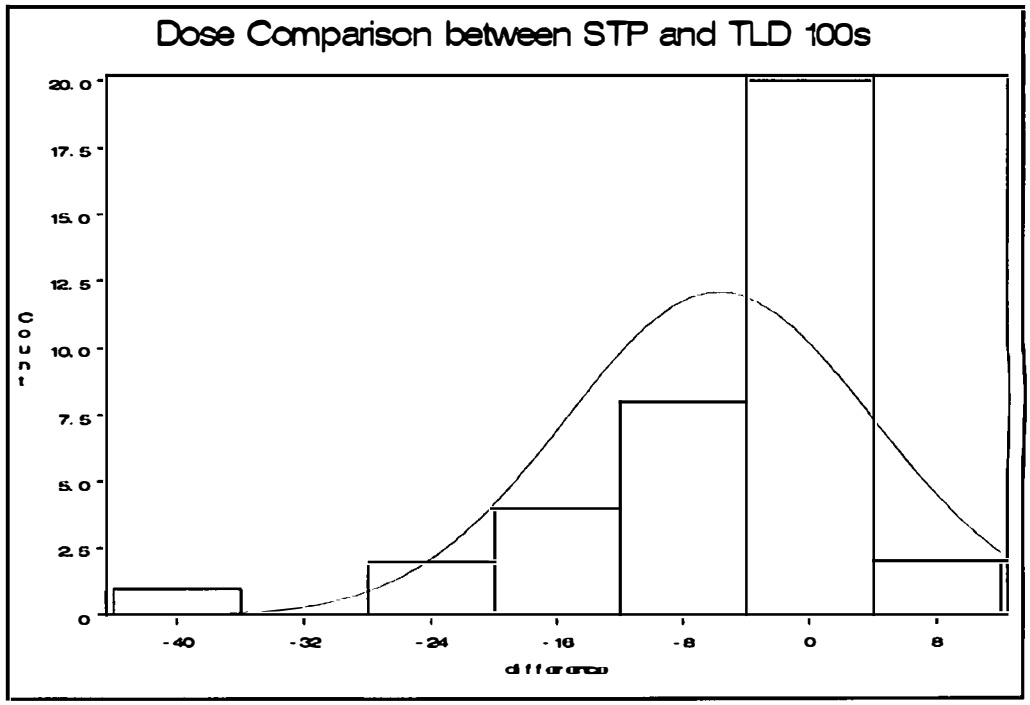

Figure 19. Distribution of the Difference between TLD-100 and TPS

These data (Table 4.1) can provide additional support in comparing the two data sets as well as determining the right methodology for pairwise comparison of the two data sets. When looking at the means of the data sets we observe that the average values for TLD 100's and the TPS are 71.8 and 77.5 cGy respectively The variances are somewhat similar as well with values of 5314.89 and 5895.91 respectively.

In general both datasets have similar distributions with similar moments and variances, and the difference between datasets appears to be small. Additional information on the SAS Code can be found in Appendix II.

To establish which paired data test to perform we must first confirm normality of the differences between the TLD-100 and the TPS (Ott & Longnecker, 2001). Graphical information on the normality is presented in Figure 19 and it is determined based on the moments, and variability of the data that normality was not fully present. With the use of a normal probability plot (Figure 20), we can visually inspect the data to verify the

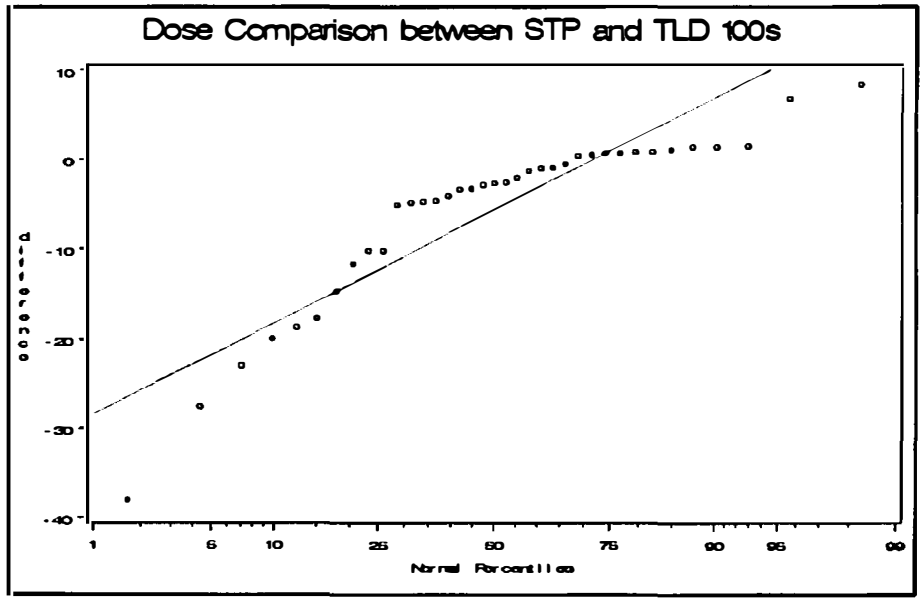

Figure 20. Normal Probability Plot of the Difference Between theTLD-100 and the TPS.

Table 4.1 Basic Statistical Measures for TLD-100, STP and their Difference

Variable: TLD100
Moments

N	37	Sum Weights	37
Mean	71.7497297	Sum Observation	2654.74
Std Deviation	72.9032646	Variance	5314.88599
Skewness	0.40117558	Kurtosis	-1.5991664
Uncorrected SS	381812.773	Corrected SS	191335.896
Coeff Variation	101.60772	Std Error Mean	11.9852229

Variable: TPS
Moments

N	37	Sum Weights	37
Mean	77.4635135	Sum Observations	2866.15
Std Deviation	76.7848584	Variance	5895.91448
Skewness	0.29779529	Kurtosis	-1.7753108
Uncorrected SS	434274.971	Corrected SS	212252.921
Coeff Variation	99.1239036	Std Error Mean	12.623353

Variable: difference

N	37	Sum Weights	37
Mean	-5.7137838	Sum Observations	-211.41
Std Deviation	9.77272547	Variance	95.5061631
Skewness	-1.538491	Kurtosis	2.45574493
Uncorrected SS	4646.1729	Corrected SS	3438.22187
Coeff Variation	-171.03772	Std Error Mean	1.60662617

normality of the difference exists and we can confirm a normal distribution, as well, with statistical tests.

Figure 20 presents a normal probability plot of the differences. In this figure we observe that the data points are not closely fitted to the normal distribution line, with a few extreme values or outliers present between -30 and -40. The figure does not show normality of the differences

For the statistical tests, SAS provides several Goodness of Fit Tests for normal Distribution Analysis. The test used in this study for normality is the Anderson-Darling Test. As expressed by Natrella *et al* the Anderson-Darling test is used to test if a sample of data came from a population with a specific distribution. The test is a modification of the Kolmogorov-Smirnov (K-S) test and gives more weight to the tails of the distribution than does the K-S test."

SAS provides these two tests in addition to other test to verify normality. The Anderson-Darling is an alternative method to using the chi square method or the Kolmogorov Method. The SAS output for testing normality of the differences between TLD-100 and the TPS is shown in Table 4.2.

Table 4.2. Tests for Normality

Test	Variable: difference --Statistic---		---------p Value---------	
Shapiro-Wilk	W	0.840656	Pr < W	<0.0001
Kolmogorov-Smirnov	D	0.255584	Pr > D	<0.0100
Cramer-von Mises	W-Sq	0.445646	Pr > W-Sq	<0.0050
Anderson-Darling	A-Sq	2.292599	Pr > A-Sq	<0.0050

*Source: *SAS*

To determine normality using the Anderson-Darling test we must determine a null hypothesis (H_0) based on a probability value (P-Value) that is compared to a significance level described as alpha (α) value based on a Type I error. A Type 1 error "is committed if we reject the null hypothesis when it is true."(Ott & Longnecker, 2001). To ensure that we are 95 % confident that the answer is correct, a α value of 0.05 is used for all tests performed for this research. SAS uses this value as a default.

The null hypothesis for the Anderson-Darling Test is that normality exists in the data distribution of the differences. The Alternative hypothesis (Ha) is that that the data are non-normal.

The test statistic (Natrella *et al*, 2004) for the Anderson-Darling Test (A^2) is:

$$A^2 = -N - S \tag{4.3}$$

where S is:
$$S = \sum_{i=1}^{N} \frac{(2i-1)}{N} [\ln F(Yi) + \ln(1 - F(Y_{N+1-i}))] \tag{4.4}$$

In Equation 4.4, F is the cumulative distribution function and Y is the ordered data for N equal to 37.

The P-Value for the Anderson-Darling in this test is less than 0.0050. Since this value is less than the α value of 0.05, the null hypothesis is rejected and we can definitively state that the distribution of the data set for the differences between the TLD-100 and the TPS is non-normal. We also observe Table 4.2 that one could have used any of the tests presented. All P values were less than 0.05.

Because the distribution of the data is non-normal, we cannot use parametric testing to perform a paired data analysis of the data between the TLD-100's and the TPS. For this study a more convenient non-parametric testing is the Wilcoxon Sign-Rank Test. This test is used as an alternative testing method to the Paired T-test when the distribution of the differences is non-normal. The Wilcoxon Sign-Rank test uses the magnitude of the rank of each data point as well as the sign of that data point in order to perform the test. This test requires that the distribution of the differences be symmetric around the median value. The hypothesis value of the median is denoted as D_0.

The Wilcoxon Sign Rank Test is performed in the following way. It first calculates the differences between the paired observations. Then, it subtracts the differences from the D_0. If any zeros are present those are removed from the data, and we have a new data set with n values minus the zero values. Finally it takes the absolute values of the differences and puts them in increasing order, which then ranks them starting with 1 though n. If there are any ties the average of the ranks is used for these ties. For the Wilcoxon Signed Rank Test the following information is pertinent:

H_o: Distribution of Differences is symmetrical around D_o (Where Do is usually 0)

Ha: Distribution of Differences is not symmetrical around Do

$\alpha = 0.05$

Test Statistic

$$z = \frac{T - \frac{n(n-1)}{4}}{\sqrt{\frac{n(n-1)(2n+1)}{24}}} \quad , \qquad (4.5)$$

where T is equal to the smaller value of the sum of the Positive Ranks (T+) or the negative Ranks (T-). N is the number of paired observations that are non-zero.

If the rejection region has values of z (Equation 4.5) less than α, the Null Hypothesis is rejected.

The results of the Wilcoxon Sign Rank Test are presented in Table 4.3. SAS by default presents three paired T test. We are interested in the last test of the table where the P- Value is 0.0004.

This value is much smaller than the alpha value of 0.05. Therefore the null hypothesis is rejected for this test, and we can conclude that the data set from the TLD-100 is different from the data set calculated by the treatment planning system software utilized for dose calculations in radiation therapy.

As expressed previously, there are some differences that take place at certain points which can be attributed to the actual location of the TLD in the phantom, inhomogeneities of the density medium as well as the actual calculation of the TPS. The calculated dose by the TPS is performed by the operator post exposure and the probability of the correct selection depends on where the operator selects the correct location of the TLD represented in the software.

Table 4.3 Paired Data Analysis between TLD-100 and TPS

Tests for Location: Mu0=0				
Test	-Statistic-		-----p Value------	
Student's t	t	-3.55639	Pr > |t|	0.0011
Sign	M	-6.5	Pr >= |M|	0.0470
Signed Rank	S	-221.5	Pr >= |S|	0.0004

Additional testing was also performed between the two distributions of the TLD and TPS to determine if they were different. Normality was analyzed and the conclusion is that neither distributions were normal; however we can determine if the variance, and the means are statistically different. To determine the differences for the means and the variance, the following tests were performed: a Levene's Test (Table 4.4) for the analysis of the variance and a T-test (Table 4.5) for analysis of the means. In order to determine analysis of means we first test for variance.

Based on this we can then determine which test to use for the means (SAS, 2001). Table 4.4 shows the SAS output for the T-test for the equality of variances, and table 4.5 shows the T-tests that can be used depending on the equality of the variances.

The Levene's test shows a P value for the equality of variances to be 0.4705. This value is less than the pre-established alpha value of 0.05. The null hypothesis fails to reject the null hypothesis and we can state that the variances of the TLD-100 and the TPS

Table 4.4: Levene's Test for Homogeneity of dose Variance Between TLD-100 and TPS

Source	DF	Sum of Squares	Mean Square	F Value	Pr > F
detector	1	5912459	5912459	0.53	0.4705
Error	72	8.0885E8	11234022		

Table 4.5: Table T-Tests for Means

Variable	Method	Variances	DF	t Value	Pr > |t|
Dose output	Pooled	Equal	72	-0.33	0.7437
Dose output	Satterthwaite	Unequal	71.8	-0.33	0.7437

show no significant differences. For variances that are equal we can use the Pool method (Table 4.5) for equal variances in order to test for equality of means. Even though the P-value shows that it exceeds the alpha of 0.05 which fails to reject the null hypothesis that the means are equal, there is still the issue of a small sample size and no normality of the data. Therefore this test might not conclusively show us that the means can be equal. By looking at the mean values there is a large difference between the means (Table 4.1).

4.4. Pairwise Comparison between the TLD-100 and the Panasonic TLD system

In addition to making a comparison between the TLD-100 and the TPS, it was of interest to compare the TLD100 with another thermoluminescent system in order to verify the reliability of the TLD-100. This portion of the study involved the radiation exposure to 25 TLD 100 and 25 Panasonic TLDs supplied by the U.S. Army Dosimetry Center. Both systems were exposed to 100 cGy imparted by the LINAC radiation therapy system at Baptist Hospital.

The statistical analysis was performed using the residual (difference) values previously presented in Table 3.4. The SAS software provided both graphical as well statistical data of the comparison between the residuals of both TLD systems. Figure 21 provides the normality distribution of the residuals of the two types of TLD's. From the figure observe that both distributions appear to be normal and with equal variability of the data. The standard deviation presented in the inset of the graphs show a value of approximately 5 (SAS Rounds off) which gives an approximate variance of 25 for both distributions. The only difference between the two distributions is the location of the

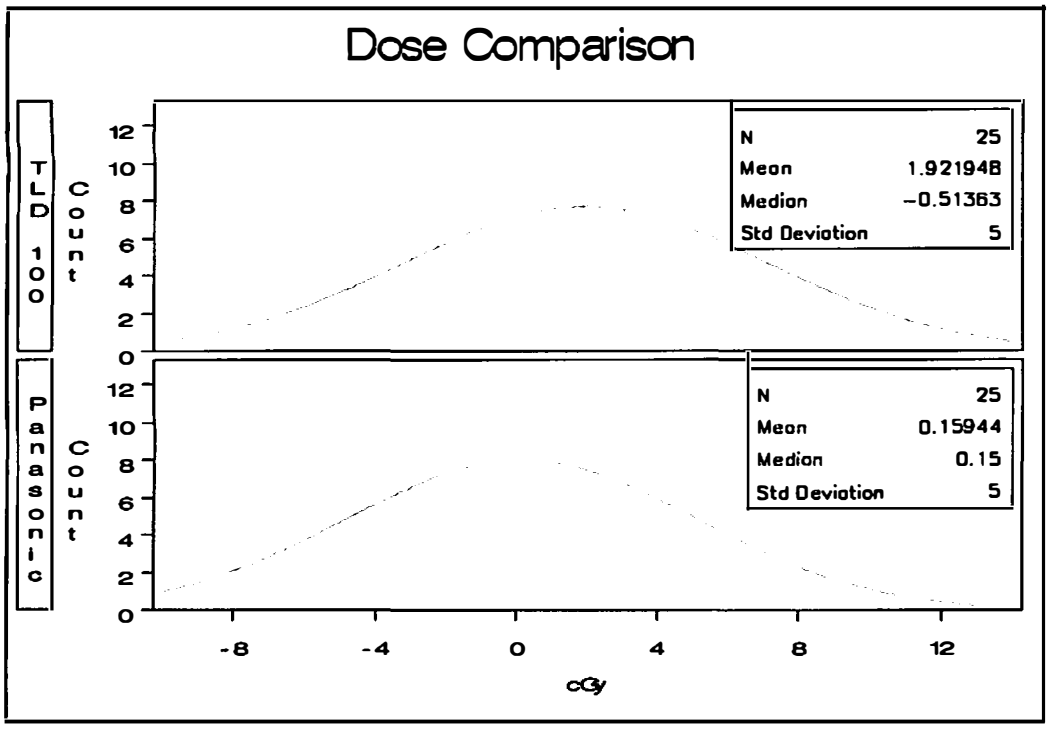

Figure 21. Normal Distribution of the Residuals of TLD-100 and the Panasonic TLD's

mean values. TLD-100 has a mean of 1.92 as compared to the Panasonic TLD's the mean is 0.15. To make a better comparison between the two distributions, SAS provides two statistical tests that can compare the variance and the means of the two sets. These tests are the Levene's Test (Table 4.6) and the Pairwise T-Test comparison test (Table 4.7). Both tests have a critical rejection region at α =0.05. Anything below this value rejects the null hypothesis that they have equal variance and equal means.

The results for these tests are shown in Table 4.6 and 4.7 respectively. For comparison of variances between the two residual distributions the P-Value is 0.8157. This P-Value is extremely large and much bigger than the critical rejection value of 0.05. Therefore there is a failure to reject the null hypothesis and one can state that there is no

Table 4.6: Levene's Test for Homogeneity of Dose Variance

Source	DF	Sum of Squares	Mean Square	F Value	Pr > F
TLD	1	54.6842	54.6842	0.05	0.8157
Error	48	47780.7	995.4		

Table 4.7: The T-TEST Procedure

Difference	DF	t Value	Pr > |t|
TLD100 - Panasonic	24	1.26	0.2183

significant difference between the variances. The P-Value for the equality of means is 0.2183. and here we fail again to reject the null hypothesis that the means are equal. There is no significant difference between the means of these two distributions. We can conclude that because of the low difference between means and the variances, both TLD systems respond to radiation in the same manner at 100 cGy.

In order to look at the efficiency of the two TLD systems we must consider the information in Table 3.4. The TLD 100 have a few outliers with values that are larger than the 5% difference from the set dose established on the LINAC system. But in general, all values seem to be less than a 5 % difference. The Army TLD's also present a small difference also with some few extreme values that exceed a 5% difference.

Based on the results presented above for dose exposure values used in this study, (between 100 and 180 cGy) the reliability and efficiency of the TLD-100s seems appropriate and comparable to the response presented by the Panasonic TLD system.

Chapter 5

Conclusions and Future Work

The objective of this study was to determine if the dose calculated by a three dimensional treatment planning system (TPS) used in radiation therapy differ by more than 5 % from actual measured dose calculations. It is the intent of oncologists and medical physicist to provide the appropriate dose to a specific malignant tumor, and at the same time for the dose to have a minimal effect on healthy tissues surrounding the tumor.

To measure the dose, Lithium Flouride (LiF:Mg:ti) thermoluminescent dosimeters (TLD's) were used. These TLD's are also known as TLD-100's. Before the actual comparison was made between the TLD-100 and the TPS, a linear dose response test and testing of the reliability of the TLD-100 were performed. It was established that neither the TLD-100 or the TLD reader have a good linear response to ionizing radiation, most particularly at doses exceeding 200 cGy. The linearity, however, at lower dose values does exist. Thus all exposures to the TLD-100 were made at values below 200 cGy.

To investigate the reliability of the TLD-100, the dose responses were compared to the dose response from the UD-802A Panasonic TLD system used by the United States Army. Twenty five TLD's from both TLD systems were exposed to 100 cGy. The dose response from both TLD systems differed by less than 5% from the set dose on the Linear Accelerator (LINAC) radiation therapy system. Additionally the dose distribution of the residual values of each TLD system were analyzed. Both systems showed normal distributions, with equal variances but different means. The TLD-100 presented a slight

left skewness. The mean for the Panasonic TLD system (μ=0.159) was closer to a mean of 0, which is what is expected when looking at residual values. The mean for the TLD-100 (μ=1.92) was a much larger. There is a possibility of a small bias, which can be attributed to several variables. One is the irregular calibration of the TLD reader. The TLD reader is used for academic purposes and it is not used on a routine basis. The other variable is that the TLD-100's have been used several times, with a potential for physical change in the TLD's or even damage.

After proper calibration of 38 TLD-100s, they were inserted into an ART phantom at the pelvic region. The ART phantom had gone through an initial mock patient treatment planning where a simulated tumor was determined in the pelvic region. After exposure of the phantom to a prescribed dose of 180 cGy, the 37 TLD dose response function was compared to the calculated dose determined by the TPS at the location of each TLD. It was found at the isocenter or the pivot point at which the central dose of 180 cGy was given, that the dose did not differ much. The nominal dose difference (NDD) between the measured dose (TLD-100) and the calculated dose (TPS) at the isocenter was 2.32 percent (Table 3.3). Other TLD's located near the isocenter maintained this pattern as well, showing NDD of less than 5 percent. For TLD's located in healthy tissues the NDD was also less than 5 %; however there were a few exceptions in locations at which there were large inhomogeneities of the medium being analyzed by the calculated dose of the TPS systems. Additional inhomogeneities can also be present in structures equivalent to bone or locations where there is an inter-phase between two different types of tissues.

In general the distributions seem to have variances with no significant difference between them (Figure 21), but they do have different mean values. To verify that the two distributions were approximately the same, several statistical methods were applied. The Anderson-Darling test was performed to verify the normality of the differences between the TLD-100 and the TPS and the equality of variances was performed using the Levene's test. Both tests showed that the differences did not show normality but does present the same variability of the data. Because the distribution of residuals was non-normal, a non-parametric test had to be applied to compare the TLD-100 and the TPS. The non-parametric test used was the Wilcoxon Sign Rank test. This test showed that the distributions of the TLD-100 and the TPS were different.

We can conclude that the measured dose was different from the calculated dose obtained from the TPS. These differences however, do not seem to be significant, showing that the larger differences took place at about 37 % of the TLD locations. The variability in the differences can be probably attributed to several factors, as mentioned before: (1) Proper calibration of TLD reader, (2) age and use of the TLD's, and (3) calculated dose by the TPS might not be appropriate for some locationa of the TLD inside the TPS system.

Future works includes performing the same experiment but usiing different TLD systems inside the ART phantom. There are other forms of TLD's that have different chemical composition and possibly have a more reliable and better linear response to ionizing radiation. Other future work that should be carried out is to expose the ART phantom at other hospitals and make a comparison between the different TPS's used at these medical institutions.

List of References

List of References

1. Tsoulfanidis, N. *Measurements and Detection of Radiation (2nd Ed).* Washington D.C.: Taylor & Frances.
2. Shultis & Faw. (2000). *Radiation Shielding.* La Grange Park: American Nuclear Society.
3. Khan, F. (1994). *The Physics of Radiation Therapy (2d Ed.).* Baltimore: Williams and Wilkens.
4. Ott R.L. & Longnecker M. (2001). *Statistical Methods and Data Analysis (5th Ed.).* Pacific Grove: Duxbery.
5. Neter J. et al.(1996). *Applied Linear Statistical Methods (3rd Ed.).* Boston: McGraw Hill.
6. Schlotzhauer S.D & Littell R.C. (1997). *SAS System for Elementary Statistical Analysis (2d Ed.).* Cary: SAS institute Corp.
7. Waligorski et al (2002). *Validation of a Radiotherapy Treatment Planning System Using An Anthropomorphic Phantom and MTS-N Thermoluminescent Dosimeters.* Radiation Protection Dosimetry 101:477-480.
8. Van Dyk J. et al (1993). *Commissioning and quality assurance of treatment planning Computers.* Int. J. Radiat. Oncol. Biol. Phys. **26** 261-273.
9. Dunscombe P. et al (1996). *Anthropomorphic Phantom measurements for the Validation of a Treatment Planning System.* Phys. Med. Biol.41. 399-411.
10. Baird C.T. et al (2001). *Verification of Tangential Breast Treatment Dose calculations in a Commercial 3D Treatment Planning System.* Journal of Applied Clinical Physics. Vol 2, No. 2. Spring 2001.
11. Gamboa-De-Buena (1998). *Thermoluminescent Response and Relative Efficiency of TLD-100 exposed to Low Energy X-Rays.* Phys. Med. Biol 43. 2073-2083.
12. Holmes M.A. *Photon Monitor Unit Calculations in Pinnacle*©. (Rev B). ADAC Laboratories. Milpitas.

13. Lochamy J. (1997). *Viability Analysis for Use in Harshaw 3500 TL Reader of TLD-100 Dosimeters and High Alumina Powdered Sand.* Analysis Report. Nuclear Engineering Dept, University of Tennessee. Knoxville.

14. Moussa, H. Thermoluminscence Dosimetry. Analysis Report. Nuclear Engineering Dept, University of Tennessee. Knoxville.

15. Natrella, Mary et al. (2004) *Engineering Statistics e-Handbook,* Gaithersburg: NIST. Retrieved June 12, 2004 at http://www.nist.gov/stat/handbook/.

16. Department of Radiation Oncology. (2004) *A Glossary of Terms for Radiation Oncology.* Philadelphia. University of Pennsylvania Health System. Retrieved June 7, 2004 at http://www.xrt.upenn.edu training/resident_glossary/html.

17. SAS® Institute. (1999) *SAS Online Doc (Version 8).* Cary: SAS® Institute

18. Saint-Gobain Ceramics and Plastics (2001). *Model 3500 Manual TLD Reader with WinRems Operator Manual (Rev B).* Solon: Radiation Measurement Products

Appendices

Appendix I

Location of TLD's in the ART Anthropomorphic Phantom.

TPS Cross-sectional View

Slice 28

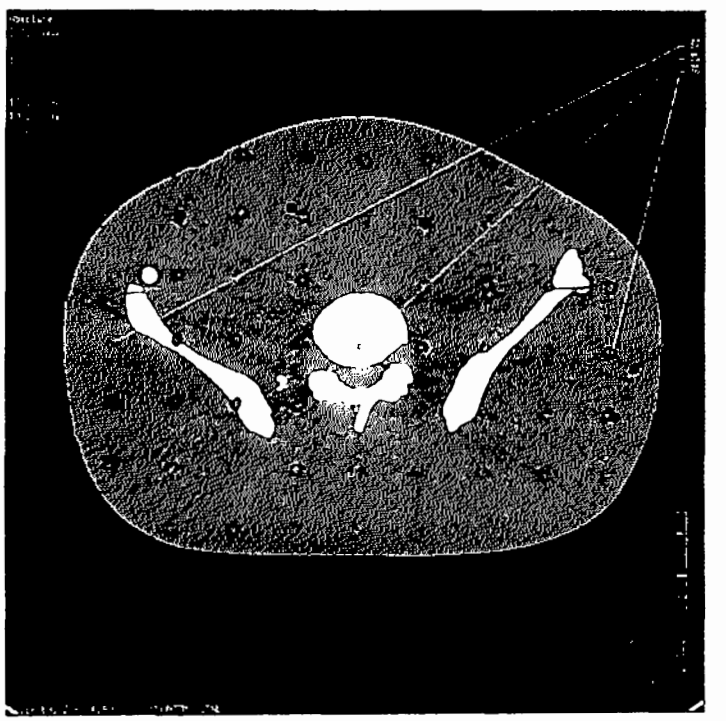

Slice 29

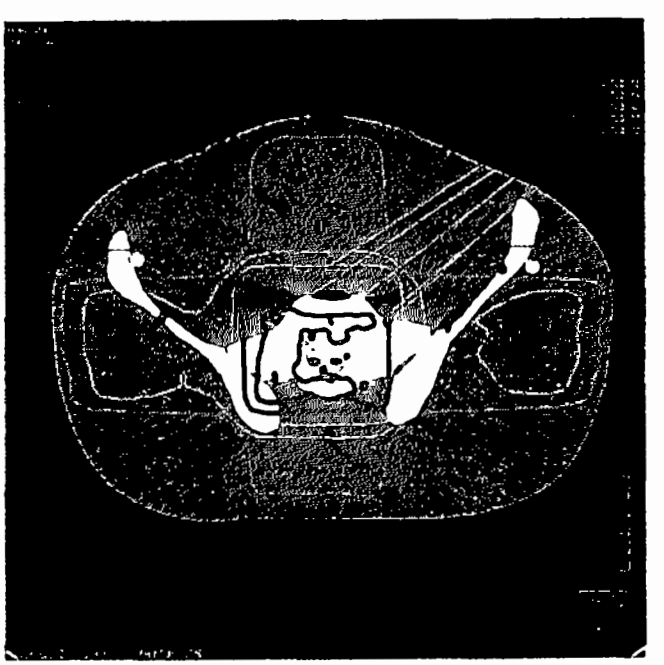

Slice 30

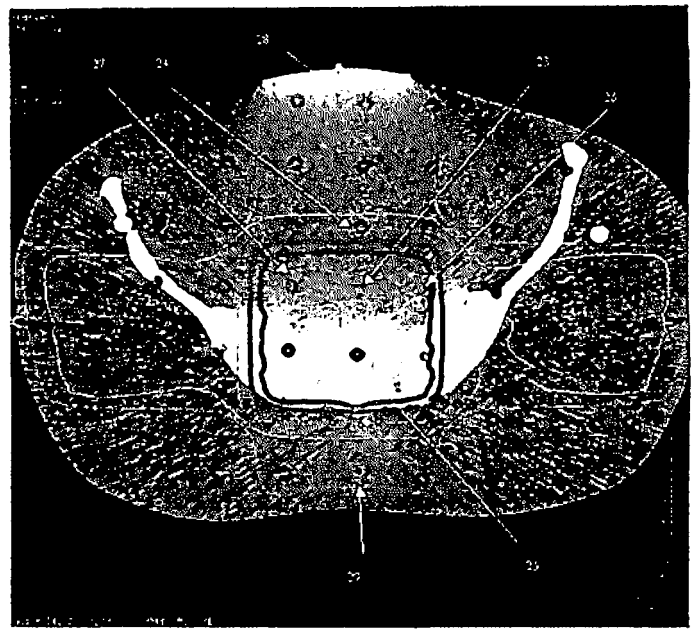

Slice 31

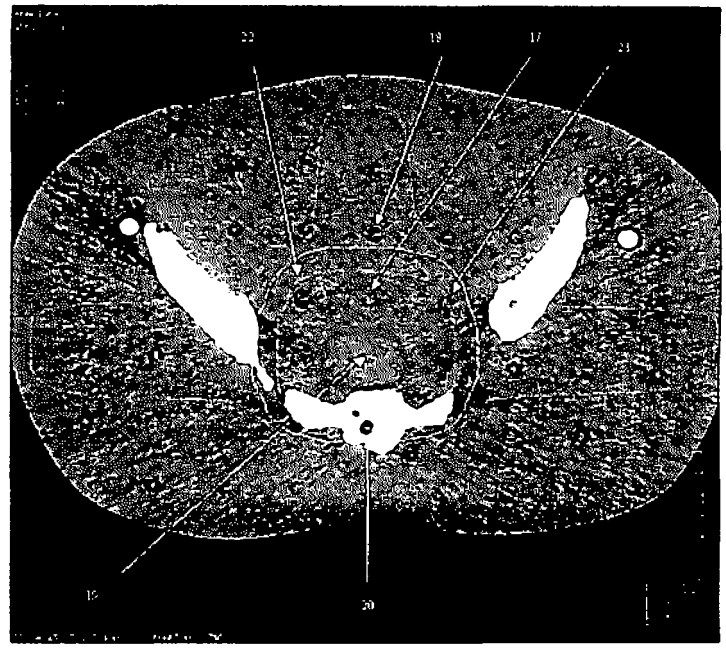

Slice 32

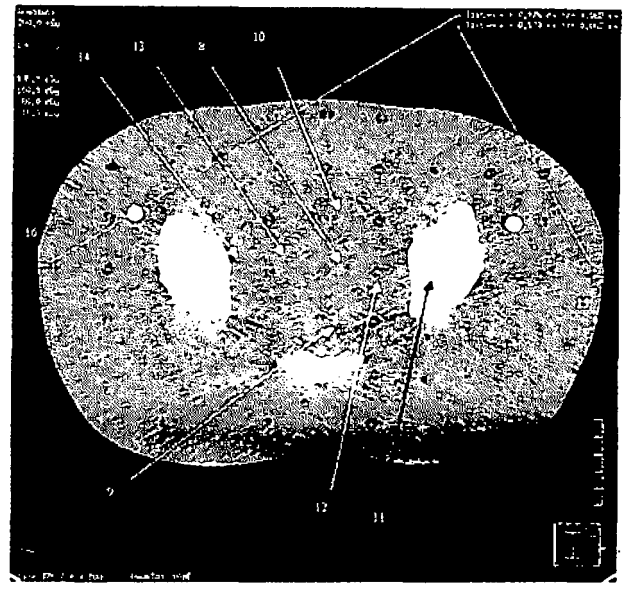

Slice 33

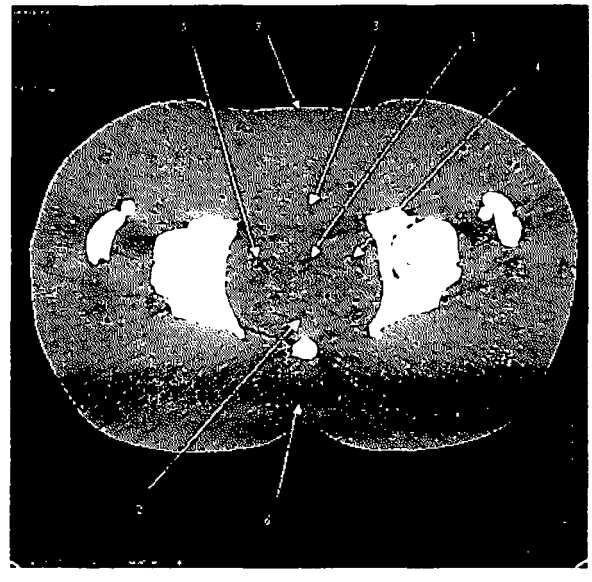

Appendix II

Statistical Analysis System (SAS) Code

1. SAS Code for Linearity of LiF:Mg:Ti using VARIAN LINAC

```
title"Dose Linearity LiF:Mg:Ti using VARIAN LINAC";
Data TLDose;
Input TLDnumb $ Doseset Dosemeas;
datalines;
1   5  5.749844369
2   5  6.022979837
3   5  6.692163354
4   5  7.114172329
5  50  58.15924226
6  50  80.81074078
7  50  74.45667940
8  50  70.17821761
9 100  107.6700052
10 100  154.5588675
11 100 145.8916715
12 100 158.6389182
13 200 207.2394751
14 200 206.3566961
15 200 225.9613043
16 200 224.4843860
17 500 580.4025189
18 500 645.8141052
19 500 869.8276168
20 500 883.9498264
21 500 917.6843150
22 1000 1387.129483
23 1000 1536.301263
24 1000 1946.102764
25 1000 1807.634208
Run;
Proc Print data= TLDose noobs;          /*Print data Set*/
Run;
symbol1 v=dot c=red height=2pct;        /*Format data points for Regression Plot*/
Proc Reg data=TLDose;
 model Dosemeas=Doseset/r clm;      /*Regression Model*/
 plot Dosemeas*Doseset;
```

plot r.*p.;
Run;
Quit;

2. SAS Code for Statistical comparison between the TLD 100 and the Panasonic TLD's

```
Options PageNo=1 NoDate FORMDLIM='*';
goptions ftext=none htext=1 cell;
options ps=60 ls=80 nodate;
  data Residual_Comparison;
     label Panasonic=' Panasonic TLD (cGy)';
       label TLD100='TLD-100 (cGy)';
     input  TLD100 Panasonic@@;
     cards;
-4.881689115 -0.478
5.716682875 -5.158
11.06530557 -8.745
-3.776830192 -7.863
-1.131571122 2.665
-2.753317979 3.824
-1.056732799 1.777
-2.41062984 1.016
-3.198958335 4.314
-1.113551673 4.416
-1.028158271 -0.845
-2.363267016 -0.845
-0.513627358 -2.406
-2.261237573 -2.406
-0.051061776 0.15
2.001459561 0.15
0.966842905 -0.169
-0.755257205 -0.169
6.303443864 1.835
9.825010532 1.835
7.370285747 -7.387
4.167227544 -7.387
5.74445893  10.113
8.500869186 10.113
13.68300163 5.636
Run;
Proc Print data=Residual_Comparison;
Run;
symbol1  c=white  v=none l=1;  /* Histogram outline */
  pattern1 c=red   v=s    r=3;
   title1 'Dose Comparison';
proc capability data=Residual_Comparison noprint graphics;
        histogram /Nobars
        midpoints=0.2 to 1.8 by 0.2
        normal (Color=Red l=1)
        legend=legend1;
     inset n mean (5.3) std='Std Dev' (5.3) skewness (5.3) /
        header = 'Summary Statistics'
        pos    = ne
```

```
        cfill  = white
        ctext  = black;
     legend1 cframe=White cborder=black;
  run;
Proc TTest Data=Residual_Comparison alpha=0.05;
 Paired TLD100*Panasonic;
Run; Quit
-------------------------------------------------------------------------------

Options PageNo=1 NoDate FORMDLIM='*';
Proc Format;
 Value det 1='TLD 100' 2='Panasonic';
 label dose='Dose (cGy)';
Run;
data TLD_Comparison;
       input  TLD dose@@;
       Format TLD det.;
     cards;
1 -4.881689115  2 -0.478
1 5.716682875  2 -5.158
1 11.06530557  2 -8.745
1 -3.776830192  2 -7.863
1 -1.131571122  2 2.665
1 -2.753317979  2 3.824
1 -1.056732799  2 1.777
1 -2.41062984  2 1.016
1 -3.198958335  2 4.314
1 -1.113551673  2 4.416
1 -1.028158271  2 -0.845
1 -2.363267016  2 -0.845
1 -0.513627358  2 -2.406
1 -2.261237573  2 -2.406
1 -0.051061776  2 0.15
1 2.001459561  2 0.15
1 0.966842905  2 -0.169
1 -0.755257205  2 -0.169
1 6.303443864  2 1.835
1 9.825010532  2 1.835
1 7.370285747  2 -7.387
1 4.167227544  2 -7.387
1 5.74445893  2 10.113
1 8.500869186  2 10.113
1 13.68300163  2 5.636
Run;
Proc Sort data=TLD_Comparison;
by TLD;
Run;
Proc Print data=TLD_Comparison;
label dose="cGy";
Run;
Proc Univariate Data=TLD_Comparison;
 Class TLD;
 label dose='cGy';
 Histogram dose / Nobars normal(color=red) VScale=Count;
 Inset N Mean Median StD (4.0)/ Position=NE;
```

```
Run;
Proc Univariate Data=TLD_Comparison Plot;
 By TLD;
 Var dose;
 ODS Select SSPlots;
Run;
Proc TTest Data=TLD_Comparison Alpha=.05;
 Class TLD;
 Var dose;
Run;
Label output='Dose (cGys)';
%Include 'E:\STATS SAS\STAT 538\SAS programs and macros\Levene.sas';
%Levene(TLD, dose, TLD_Comparison);
```

3. Dose Comparison between the TLD-100 and the TPS

```
Options PageNo=1 NoDate FORMDLIM='*';
Title 'Dose Comparison between STP and TLD 100s';
Data Dosecomp;
 Input TLD100 TPS;
      difference=TLD100-TPS;
 DataLines;
2.94 2.18
2.67 2.11
2.86 1.78
2.54 2.20
3.03 2.28
2.77 1.88
2.33 1.48
8.13 11.05
8.15 12.85
7.57 8.48
5.20 5.72
6.15  8.85
6.96  9.58
5.05  6.28
5.23  3.80
4.52  3.18
136.48 159.47
144.80 172.40
81.90 92.20
90.89 128.90
142.86 146.20
124.19 138.90
180.73 184.90
110.80 128.50
162.88 182.80
167.61 177.90
173.07 184.70
83.59 88.67
88.79 87.40
180.00 180.80
115.45 134.10
```

```
178.38 180.50
179.67 173.00
189.52 181.10
24.52 29.13
11.48 16.38
11.03 14.50
Run;
Proc Print data=Dosecomp;
Run;
Proc Sort data=Dosecomp;
by TLD100;
Run;
Symbol V=square H=.5;
Proc univariate data=Dosecomp Normal Plot;
VAR TLD100 TPS Difference;
QQplot TLD100 TPS/normal(mu=est sigma=est color=red L=1);
INSET MEAN STD/CFILL=BLANK FORMAT=5.2;
Histogram TLD100 TPS Difference/normal vscale= Count;
Probplot TLD100 TPS Difference / Normal(mu=est sigma=est) PctlMinor;
RUN;
Symbol V=square color=green H=.5;
Proc TTest Data=Dosecomp alpha=0.05;
 Paired TLD100*TPS;
Run;
Proc Univariate Data=Dosecomp;
 Var Difference;
 ODS Select TestsforLocation;
Run;
Proc Univariate Data=Dosecomp noprint;
Var Difference;
Output out=answers n=N Mean=Xbar stdmean=SE t=t Probt=P
signrank=Wilcoxon
      probs=P_Wilcoxon Normal=N_test probn=P_Normal;
        Proc Print data=answers;
        run;

-------------------------------------------------------------------------------------------------------

Options PageNo=1 NoDate FORMDLIM='*';
Proc Format;
 Value det 1='TLD 100' 2='Treat. Planning System';
Run;
data Dosecalc;
      input detector output@@;
Format detector det.;
datalines;
1 2.94  1 2.67  1 2.86  1 2.54  1 3.03  1 2.77  1 2.33 1 8.13  1 8.15
1 7.57  1 5.20  1 6.15 1 6.96
1 5.05  1 5.23  1 4.52   1 136.48  1 144.80  1 81.90  1 90.89  1 142.86
1 124.19  1 180.73 1 110.80
1 162.88  1 167.61  1 173.07  1 83.59  1 88.79  1 180.00  1 115.45  1
178.38  1 179.67  1 189.52
1 24.52  1 11.48  1 11.03
```

```
2 2.18  2 2.11  2 1.78  2 2.20  2 2.28  2 1.88  2 1.48  2 11.05  2
12.85  2 8.48  2 5.72  2 8.85  2 9.58
2 6.28  2 3.80  2 3.18  2 159.47  2 172.40  2 92.20  2 128.90  2 146.20
2 138.90  2 184.90  2 128.50
2 182.80  2 177.90  2 184.70  2 88.67  2 87.40  2 180.80  2 134.10  2
180.50  2 173.00  2 181.10
2     29.13  2 16.38  2 14.50
;

Run;
Proc Print data = Dosecalc noobs;
Run;
Proc Univariate Data=Dosecalc;
 Class detector;
 Histogram output / normal VScale=Count;
 Inset N Mean Median StD (4.0)/ Position=NE;
Run;
Proc Univariate Data=Dosecalc Plot;
 By detector;
 Var output;
 ODS Select SSPlots;
Run;
Proc TTest Data=Dosecalc Alpha=.05;
 Class detector;
 Var output;
Run;
%Include 'E:\STATS SAS\STAT 538\SAS programs and macros\Levene.sas';
%Levene(detector, output, Dosecalc);
```

Vita

Carlos E. Corredor was born in Athens, Tennessee on August 11, 1958. Son of Carlos F. Corredor and Shirley M. Buckner, Carlos was raised and educated in both the United States and in the country of Colombia, South America. Carlos is married to Luz Adriana and has two children, Christopher 22, and Ana Milena, 13 years old.

Mr. Corredor earned an Associate in Arts in Math & Science in 1991, from the University of South Carolina. Upon moving to Texas he completed his Bachelors of Science in Applied Sciences with a specialty in Radiation Safety. The degree was awarded from the University of Central Texas in 1995, a division of the Texas A&M educational system.

Mr. Corredor has worked in the field of Health Physics over 10 years with the United States Army. Mr. Corredor still remains on active duty and has worked with this this federal institution for 17 years. Mr. Corredor is a Captain in the U.S. Army and has held duties as an Alternate Radiation Safety Officer, Radiation Safety Officer, passing three Nuclear Regulatory Commission (NRC) Inspections at two military hospitals. Mr. Corredor served as well as consultant for issues related to Chemical, Biological, Radiological, Nuclear and Energy (CBRNE) for the Army, and other military branches in the Department of Defense.